An agent-based model that simulates the spatio-temporal dynamics of sources and transfer mechanisms contributing faecal indicator organisms to streams. Part 1: Background and model description

Aaron J. Neill[a,b], *Doerthe Tetzlaff*[c,d,a], *Norval J.C. Strachan*[e], *Rupert L. Hough*[b], *Lisa M. Avery*[b], *Sylvain Kuppel*[f,g,a], *Marco P. Maneta*[h], *Chris Soulsby*[a,c]

[a] Northern Rivers Institute, University of Aberdeen, Aberdeen, AB24 3UF, Scotland, United Kingdom.

[b] The James Hutton Institute, Craigiebuckler, Aberdeen, AB15 8QH, Scotland, United Kingdom.

[c] IGB Leibniz Institute of Freshwater Ecology and Inland Fisheries, 12587 Berlin, Germany.

[d] Department of Geography, Humboldt University Berlin, 10099 Berlin, Germany.

[e] School of Biological Sciences, University of Aberdeen, Cruickshank Building, St Machar Drive, Aberdeen, AB24 3UU, Scotland, United Kingdom.

[f] Institut de Physique du Globe de Paris, CNRS UMR 7154 - University of Paris, 75231 Paris, France.

[g] INRAE, RiverLy, 69625 Villeurbanne, France.

[h] Geosciences Department, University of Montana, Missoula, MT 59812-1296, USA.

Corresponding Author

Aaron J. Neill

aaron.neill@abdn.ac.uk

Northern Rivers Institute, University of Aberdeen, Aberdeen, AB24 3UF, Scotland, United Kingdom.

Highlights

- Present a new agent-based model for simulating faecal indicator organisms (FIOs).
- Simulates fate and transport of agents representing a sufficient sample of FIOs.
- Models loading, die-off, detachment, surface routing, seepage and channel routing.
- Hydrological environment is generated by a robustly-constrained hydrological model.
- Present EcH_2O-iso as an appropriate hydrological environment generator.

Abstract

A new Model for the Agent-based simulation of Faecal Indicator Organisms (MAFIO) is developed that attempts to overcome limitations in existing faecal indicator organism (FIO) models arising from coarse spatial discretisations and poorly-constrained hydrological processes. MAFIO is a spatially-distributed, process-based model presently designed to simulate the fate and transport of agents representing FIOs shed by livestock at the sub-field scale in small (<10 km^2) agricultural catchments. Specifically, FIO loading, die-off, detachment, surface routing, seepage and channel routing are modelled on a regular spatial grid. Central to MAFIO is that hydrological transfer mechanisms are simulated based on a hydrological environment generated by an external model for which it is possible to robustly determine the accuracy of simulated catchment hydrological functioning. The spatially-distributed, tracer-aided ecohydrological model EcH_2O-iso is highlighted as a possible hydrological environment generator. The present paper provides a rationale for and description of MAFIO, whilst a companion paper applies the model in a small agricultural catchment in Scotland to provide a proof-of-concept.

Key words:

Diffuse pollution; *E. coli*; EcH_2O-iso; Microbial water quality; Tracer-aided modelling; Water quality modelling

1 Introduction

Transfer of faecal pathogens (e.g. *E. coli* O157) to water bodies represents a significant risk to public health, with the ingestion of contaminated water through drinking or recreational use having the potential to cause severe gastrointestinal illness in humans (Fewtrell and Kay, 2015; Oliver et al., 2005a). Faecal indicator organisms (FIOs), such as generic *E. coli*, are commonly used to monitor microbial water quality and indicate the potential presence of pathogens which are more difficult to quantify directly (Geldreich, 1996). Risk of impaired microbial water quality is often elevated in agricultural catchments due to the large range of FIO sources that are present (e.g. different livestock) and the multiple transport mechanisms (e.g. overland flow, seepage from areas of degraded soil) that can transfer FIOs to streams (Chadwick et al., 2008). Successful implementation of mitigation measures in such environments requires the spatio-temporal dynamics of sources and transfer mechanisms contributing FIOs to streams at the sub-field scale to be understood (Oliver et al., 2007, 2016; also c.f. Greene et al., 2015; Vinten et al., 2017). This likely requires the integration of empirical data with process-based FIO models (de Brauwere et al., 2014); however, uncertainties over the robustness of hydrological processes simulated by such models and the coarse spatial discretisation they often employ may hinder their use in understanding the sub-field-scale drivers of in-stream FIO dynamics that emerge at the catchment scale (c.f. Rode et al., 2010; Wellen et al., 2015).

The overall aim of this paper is to outline a new Model for the Agent-based simulation of Faecal Indicator Organisms (MAFIO); it is structured as follows. Section 2 reviews the pertinent limitations of existing process-based FIO models before exploring how agent-based and tracer-aided modelling approaches have potential in helping these to be addressed. This provides the rationale for the development of MAFIO, which simulates the sub-field-scale fate and transport of agents representing FIOs in a spatially-distributed and process-based manner, underpinned by a hydrological environment generated by a robust hydrological model. A detailed model description is presented in Section 3. Finally, Section 4 introduces the tracer-aided ecohydrological model EcH$_2$O-iso (Kuppel et al., 2018a) as a potential example of a robust hydrological environment generator and details its coupling to MAFIO. A companion paper (Neill et al., *in review*) provides a proof-of-concept application of MAFIO focusing on process representation and the model's potential for use in a management context.

2 Rationale for model development

2.1 Current limitations to simulating sources and transfer mechanisms contributing FIOs to streams at the sub-field scale

A prerequisite to using models to understand the drivers of dynamics in water quality parameters is proper constraint of processes to which the parameters may be sensitive (Sokolova et al., 2018; Vaché and McDonnell, 2006). For microbial water quality, hydrological processes are often hypothesised as a major control on observed FIO dynamics (Kay et al., 2008; Oliver et al., 2005a; Tetzlaff et al., 2012). However, catchment hydrological functioning in process-based FIO models can often only be constrained through calibration to discharge data from a catchment outlet (Cho et al., 2016). Such data primarily capture the speed at which perturbations (e.g. rainfall) to the system are transmitted through the catchment, with limited insight into internal catchment states and fluxes (Birkel et al., 2014a; McDonnell and Beven, 2014). Consequently, flow path dynamics and resulting hydrological connectivity are likely to be poorly constrained in FIO models, potentially undermining their ability to accurately represent hydrological mechanisms that transfer FIOs to streams (c.f. Sokolova et al., 2018; Vaché and McDonnell, 2006; Wellen et al., 2015).

A further issue is coarse spatial discretisation in many process-based FIO models, with lumped (e.g. Haydon and Deletic, 2006; Neill et al., 2019) to semi-distributed (e.g. Sadeghi and Arnold, 2002; Whitehead et al., 2016) model structures generally being the norm. Whilst limited examples of fully-distributed FIO models do exist, they have often been implemented at coarse resolutions (e.g. the 1 km^2-resolution WATFLOOD model of Dorner et al., 2006). Consequently, the spatial discretisation adopted by many FIO models is often inconsistent with the scales at which heterogenity in hydrological processes and FIO fate and transport is expressed, and at which mitigation measures can be implemented (c.f. Fatichi et al., 2016; Rode et al., 2010; Wellen et al., 2015).

Recent progress in spatially-distributed tracer-aided modelling has potential in simultaneously overcoming issues of scale and hydrological process realism in FIO models (see Section 2.3). However, spatially-distributed simulation of FIO dynamics alone is unlikely to be sufficient for fully understanding sources and transfer mechanisms contributing FIOs to streams; this requires explicit tracking of FIOs as they move through a catchment. As summarised by Reaney (2008), spatially-distributed models conventionally simulate fluxes into and out of individual grid cells, but no information is available on the spatial origin of the constituents (water/contaminants) comprising those fluxes; consequently, it is often only possible to simulate the locations of active fluxes and what their magnitude is, but not actually whether those fluxes contribute water/contaminants to the stream. A possible solution, which could also have value in simulating the heterogenous behaviour of FIOs of different types or from different host animals (e.g. die-off kinetics: Avery et al., 2004), is the incorporation of agent-based methods into spatially-distributed modelling frameworks (Reaney, 2008).

124 *2.2 The potential of agent-based modelling approaches*

125 Agent-based models (ABMs) comprise three major elements: 1) agents representing autonomous
126 individuals, each associated with a set of attributes and the ability to sense and process information
127 regarding their surroundings; 2) a simulation environment that can be distributed in space in which the
128 agents operate; 3) a set of rules, conditional or stochastic in nature, defining how agents interact with
129 the environment and with each other based on their attributes (Abdou et al., 2012; Crooks and
130 Heppenstall, 2012). Agent attributes can relate to any characteristic necessary to simulate the
131 behaviours of the phenomena being studied or that is of interest for the problem being addressed (Macal
132 and North, 2010). Whilst often more demanding than aggregative modelling approaches in terms of
133 computation, data requirements and evaluation, the bottom-up approach of ABMs allows greater scope
134 for representing heterogeneity amongst individual agents and their interactions with the simulation
135 environment, permitting richer simulation of small-scale behaviours and how these cause higher-level
136 system dynamics to emerge (O'Sullivan et al., 2012).

137

138 Use of ABMs for the process-based simulation of water quantity/quality dynamics has been relatively
139 limited. However, there are promising examples of the development of such models to elucidate spatio-
140 temporal patterns of surface hydrological connectivity through tracking locational attributes of agents
141 representing water particles as they move through catchments (Reaney, 2008), and to simulate the
142 hydrologically-induced erosion and transport of markers (similar to agents) representing sediment
143 particles based on their unique characteristics (Cooper et al., 2012). Furthermore, several studies have
144 successfully implemented closely-related yet simpler (Crooks and Heppenstall, 2012) cellular automata
145 models to simulate hydrological processes (e.g. Cirbus et al., 2013; Hodge and Hoey, 2012; Ravazzani
146 et al., 2011; Shao et al., 2015). Consequently, representing FIOs as agents within an ABM could have
147 significant potential for simulating their fate and transport, with agent attributes governing how they
148 interact with different transfer mechanisms operating in a simulated environment and permitting their
149 pathways through catchments to be tracked.

150

151 *2.3 Progress in spatially-distributed, tracer-aided (eco)hydrological modelling*

152 The dynamics of stable isotopes (^{2}H and ^{18}O) in streamwater contain information with respect to the
153 velocities of water passing through a catchment, as influenced by factors such as hydrological
154 connectivity, storage and mixing (Birkel and Soulsby, 2015; McDonnell and Beven, 2014).
155 Consequently, incorporation of isotopes as tracers into hydrological models allows performance
156 assessments to advance from how well a model fits an observed hydrograph, to also how consistent the
157 model is with internal catchment processes giving rise to the velocity response (Birkel et al., 2014a;

McDonnell and Beven, 2014). Improved confidence in the realistic simulation of catchment functioning afforded by such tracer-aided hydrological models has facilitated their use in providing valuable insights into how catchments store and release water (Birkel and Soulsby, 2015), and how these factors drive various water quality parameters including dissolved organic carbon (Birkel et al., 2014b; Dick et al., 2015) and FIOs (Neill et al., 2019). Recently, tracer-aided models have evolved from their early lumped conceptual structures towards ones that are fully-distributed and increasingly physically-based (e.g. Kuppel et al., 2018a; Remondi et al., 2018; van Huijgevoort et al., 2016), reflecting cheaper isotope analysis (e.g. Berman et al., 2013) and recognition of the need for catchment systems to be modelled in this way to tackle issues of water quality and environmental change (Fatichi et al., 2016). Such models have permitted more nuanced simulation of catchment-scale discharge and tracer dynamics, and also facilitate specific interrogation of intra-catchment water and isotope dynamics to further increase confidence that internal catchment processes are being correctly represented (Ala-aho et al., 2017; Knighton et al., 2020; Kuppel et al., 2018a; Piovano et al., 2018, 2019; Remondi et al., 2018; Smith et al., 2019).

In addition to the value of tracers, the importance of resolving how water is partitioned between "green" (evaporation and transpiration) and "blue" (discharge and groundwater recharge) hydrological fluxes when representing the storage and release of water by catchments is increasingly recognised (Brooks et al., 2015; Falkenmark and Rockström, 2006). Most tracer-aided models only explicitly simulate "blue" fluxes, with "green" fluxes specified as a combined variable usually partitioned based on model parameters (Fatichi et al., 2016; Vivoni, 2012). However, tracer-aided ecohydrological models are emerging that explicitly resolve both "blue" and "green" fluxes whilst also simulating stable isotope dynamics to enable further evaluation of process consistency (Kuppel et al., 2018a; Maneta and Silverman, 2013). Such a model, EcH_2O-iso (Kuppel et al., 2018a), is introduced in Section 4 as an example of a hydrological environment generator for MAFIO. However, it is stressed that any model can be used, providing it can be robustly determined as to whether catchment hydrological functioning is being successfully captured.

3 Presentation of *MAFIO*

This presentation follows the ODD (Overview, Design Concepts, Details) protocol for describing agent-based models (Grimm et al., 2006, 2010). MAFIO is written in the Python 3.6 programming language and makes use of the PCRaster module (Karssenberg et al., 2010) for handling spatial inputs and outputs. Given that it can be coupled with any robust hydrological model that provides the necessary

outputs, the following presentation of MAFIO is provided in a generic form, with Section 4 outlining the specific interfacing with EcH_2O-iso.

3.1 Purpose

The purpose of this initial version of MAFIO is to reveal the spatio-temporal dynamics of sources and transfer mechanisms contributing FIOs to streams at the sub-field scale in small (< 10 km^2) agricultural catchments. This is achieved by simulating and tracking, in a spatially-distributed, process-based manner, the fate and transport of agents representing FIOs shed by different types of livestock (Figure 1).

3.2 State variables and scales

MAFIO consists of four entities. Two environments drive the simulation: a catchment environment and a hydrological environment. These set the attributes of a spatial grid on which simulations take place over discrete timesteps. The behaviour of agents representing FIOs (FIO-agents) is then simulated based on their individual attributes and those of the spatial grid for each timestep.

3.2.1 Catchment environment

The catchment environment defines, on a regular grid, the following fixed spatial characteristics of the catchment being modelled:

1) Spatial extent;
2) Distribution of land parcels, that may be delineated based on land uses (e.g. pastoral field, arable field) or covers (e.g. forest, moorland);
3) Local flow direction based on the D8 algorithm (O'Callaghan and Mark, 1984);
4) Location and width of the stream channel;
5) Locations where soil is degraded adjacent to the channel;
6) Grid cells immediately upslope of those containing a channel;
7) Grid cells immediately upslope of those containing degraded soil;
8) Vertical discretisation of the landscape, currently limited to the land surface and the first few centimetres of the upper soil profile (exact depth unspecified) where it is assumed most interactions of FIOs with the soil will occur (Stocker et al., 2015).

Additionally, counts of each livestock type (e.g. sheep, cattle) considered in the simulation for each land parcel, and which areas of the stream are accessible to livestock, are specified, both of which vary in time.

3.2.2 Hydrological environment

The hydrological environment (Figure 2) is provided by a spatially-distributed hydrological model that can simulate the following on a regular spatial grid: effective precipitation (P_{Eff}), effective solar radiation (SR_{Eff}), ponded surface water prior to infiltration (*Pond*), infiltration flux (*Infil*), soil water content prior to exfiltration (SWC_{Exf}), exfiltration flux (*Exfil*), soil saturation deficit (scaled between 0 for fully saturated and 1 for only residual soil moisture present; Sat_{Def}) and soil skin temperature (T_{Skin}). Here, effective precipitation is total precipitation minus interception, whilst effective solar radiation is that absorbed by the ground after accounting for transmission and reflective losses. Whilst not explicitly part of the hydrological environment, run-on and run-off are accounted for implicitly by assuming that any water remaining on the surface following infiltration/exfiltration runs off to contribute to *Pond* of the next downslope grid cell (consistent with EcH$_2$O-iso). The hydrological environment gives the following abstract conceptualisation of catchment hydrological functioning from the perspective of MAFIO (Figure 2). For a given grid cell, there are two hydrological stores: Ponded Surface Water and Soil Water. First, P_{Eff} and run-on from upslope cells enter Ponded Surface Water to define *Pond*. Water can then infiltrate (*Infil*) into Soil Water to increase SWC_{Exf} and reduce Sat_{Def}, after which water can exfiltrate (*Exfil*) back to Ponded Surface Water if the soil is now saturated (i.e. $Sat_{Def} = 0$). Finally, any remaining water in Ponded Surface Water is routed to the next downslope cell unless a channel is present, in which case remaining water is routed to the stream and out of the catchment. It should be noted that this conceptualisation only includes stores and fluxes of water relevant to the transport of FIOs in naturally-drained environments; however, future iterations of MAFIO may look to allow for artificial drainage as a potentially-efficient FIO transport pathway (Oliver et al., 2005b).

3.2.3 Timestep

MAFIO operates on discrete timesteps consistent with the fixed temporal resolution of variables defined by the aforementioned environments. Here, a daily timestep is used. However, if needed to account for non-linearities in observed FIO dynamics (McKergow and Davies-Colley, 2010), sub-daily timesteps could be used with appropriate changes to parameter values and sufficient computing power.

3.2.4 Spatial grid

Simulations take place on a regular spatial grid (Figure 1), with each grid cell having fixed and dynamic attributes (Table 1). The catchment environment determines values of fixed attributes. The position of a cell within the environment (*X-Y location* [Loc_{Att}]) determines values for *Channel cell* ($chan_{Att}$), *Flow direction* ($fDir_{Att}$), and *Land parcel(s)* (LP_{Att}). Multiple land parcels can be specified for a cell containing a channel to indicate those on either side of the channel. The attribute *Cell size* ($size_{Att}$) is determined by the spatial resolution of the catchment and hydrological environments. However, to allow for spatial resolutions too coarse to resolve small channels (Zhang and Montgomery, 1994) and processes occurring at the land-water interface that are possibly crucial for water quality (e.g. Karr and Schlosser, 1978), sub-grid heterogeneity can be represented in cells containing a channel. These have the additional fixed attributes *Proportion of cell area occupied by channel* (P_Chan_{Att}) and *Degraded soil in cell* ($degSoil_{Att}$), to allow for the channel not occupying the whole cell and the presence of degraded soil in the vicinity of the channel from livestock compaction, respectively. The latter may result in the chronic seepage of water and FIOs to the stream (Bilotta et al., 2007). P_Chan_{Att} is calculated by multiplying the width and straight-line length (*streamDist*, equal to either $size_{Att}$ *or* $[2 \times size_{Att}^{2}]^{0.5}$ depending on $fDir_{Att}$) of the channel occupying a cell, then dividing by cell area.

The dynamic attributes of the spatial grid are calculated for each timestep. They are predominantly derived from the hydrological environment (Figure 3) and are largely responsible for the behaviour of FIO-agents before entering the channel. *Effective precipitation* (P_{Att}), *Effective solar radiation* (SR_{Att}) and *Soil skin temperature* (TS_{Att}) are equal to P_{Eff}, SR_{Eff} *and* T_{Skin}, respectively. The attributes *Probability of exfiltration* (P_Exfil_{Att}) and *Probability of infiltration* (P_Infil_{Att}) are defined as:

$$P\_Exfil_{Att} = \frac{Exfil}{SWC_{Exf}} \qquad Eq.1$$

$$P\_Infil_{Att} = \frac{Infil}{Pond} \qquad Eq.2$$

Figure 3a gives a visual example of how hydrological environment variables translate to attributes of the spatial grid. Since sub-grid heterogeneity is represented in MAFIO but not necessarily in the hydrological environment simulator, dynamic attributes of cells containing a channel may need derivation from variables simulated for neighbouring cells. This could involve taking average values from upslope cells which drain into the cell in question (Figure 3a); conceptually, this implies that the land surface adjacent to the channel implicitly represented in MAFIO is an aggregated extension of the upslope cells.

The attribute *Probability of seepage* (P_Seep_{Att}) uses variables of the catchment and hydrological environments to encapsulate the combined effects of livestock grazing pressure and soil moisture on soil degradation (Drewry, 2006) and the associated potential for FIO seepage into streams (Bilotta et al., 2007; Tetzlaff et al., 2012). To indicate livestock grazing pressure, livestock count(s) for the present timestep for land parcels(s) associated with cells containing degraded soil are converted into livestock units per hectare (LU ha^{-1}; Natural England, 2013). This variable is then classified into a band ("low", "medium" or "high" - see Section 3.7.2.4) tied to a certain fraction of soil that could be degraded on the current timestep (D_{frac_new}; c.f. Sheath and Carlson, 1998); if no livestock are present, D_{frac_new} is 0. However, since soil takes time to recover once degraded, the final fraction of degraded soil (D_{frac}) used for the timestep is the maximum of D_{frac_new} and the damage fraction of the previous timestep (D_{frac_old}) subjected to exponential decay (Figure 3b; c.f. Elliot et al., 2002); the latter occurs at a rate specified by the parameter k_d in units of T^{-1}, where T is the length of a timestep:

$$D_{frac} = \max\left\{D_{frac_{new}}, D_{frac_{old}}.e^{-k_d T}\right\} \qquad Eq.3$$

The value of D_{frac} is then scaled by the average Sat_{Def} of cells immediately upslope (as cells with degraded soil also contain a channel) to account for the impact of moisture content in the extent of soil degradation (Drewry, 2006), and to give the final probability of seepage (Figure 3b):

$$P\_Seep_{Att} = D_{frac}.\left(1 - Sat_{Def}\right) \qquad Eq.4$$

3.2.5 FIO-agents

FIOs in MAFIO are represented by FIO-agents. Given likely large numbers of FIOs present within agricultural catchments, it is impossible for each FIO to be represented by a single FIO-agent. Consequently, MAFIO initially adopts the simple approach of assuming that the overall behaviour of a population can be inferred from simulating a suitably-sized sample (Parry and Bithell, 2012; Reaney, 2008). FIO-agents are characterised by dynamic, fixed and memory attributes (Table 2). Dynamic attributes can be updated multiple times within a timestep due to die-off and transport processes. *Attached-stream sediment* and *Detached-faeces* indicate whether an FIO-agent is attached to stream sediment or detached from a faecal deposit, respectively. The former determines how the FIO-agent is routed through the stream, whilst the latter specifies whether an FIO-agent is available for transport.

Domain type accounts for the position of the FIO-agent at the sub-grid scale (either in a cell without a channel or otherwise its location within a cell containing a channel). *Infiltration stage* denotes where in the vertical discretisation of the catchment the FIO-agent is, which will affect the die-off and transport processes it can experience. *Life state* and *Movement tracker* follow whether the FIO-agent is alive or dead (to determine whether it is still tracked) and if the FIO-agent moved in the current timestep, respectively. Finally, *Timestep*, *X co-ordinate* and *Y co-ordinate* specify the current timestep, and X and Y co-ordinates of the FIO-agent; these allow recording of when changes to certain dynamic attributes occur in the simulation and where in the spatial grid the FIO-agent is situated. Memory attributes keep track of how dynamic attributes of the FIO-agents change over the simulation; this permits tracking of, for example, the origin of an FIO-agent that reaches the stream or the path that it took to the stream. Fixed attributes are assigned when the FIO-agent spawns and record its original host animal (*Livestock type)* and the land parcel into which it spawned (*Land parcel*). At present, MAFIO is configured to consider only a single type of FIO (*E. coli*); however, an additional fixed attribute for FIO-agents specifying their FIO type could easily allow representation of multiple FIO types with specific parameterisations.

3.3 Process overview and scheduling

Process scheduling during each timestep is shown in Figure 4a. First, environmental variables define dynamic attributes of the spatial grid, which is loaded in. Next, the Defecation Sub-model (Section 3.7.1) simulates FIO loading by spawning FIO-agents in each land parcel in a set order, based on their associated livestock counts. When new FIO-agents are spawned, their fixed attributes and initial values for dynamic attributes are set. Next, for each FIO-agent in turn (Figure 4b), behaviours resulting from fate and transport processes operating at the sub-field scale during the current timestep are simulated via the small-scale behaviour sub-models (Section 3.7.2). Once the behaviour of all FIO-agents has been simulated, those with *Life state* = 0 are removed during a "clean-up" operation, before the spatio-temporal outputs for the current timestep are finally saved (Figure 4a).

For each FIO-agent, the sequence of small-scale behaviour sub-models that runs depends on certain attribute values (Figure 4b), and may include Die-off (Section 3.7.2.1; Figure 5), Detachment (Section 3.7.2.2; Figure 6), Surface Routing (Section 3.7.2.3; Figure 7), Seepage (Section 3.7.2.4; Figure 8) and Channel Routing (Section 3.7.2.5; Figure 9). As indicated in Figures 5-9, different sub-models utilise various attributes of the spatial grid as input and have the potential to update the dynamic and associated memory attributes of the FIO-agent. Memory attributes are also updated for the start of a new timestep if the FIO-agent was already present in the model domain (Figure 4b). There are six conditions that will cause MAFIO to move on to simulate the next FIO-agent: 1) the Die-off Sub-model results in the FIO-

agent dying; 2) the FIO-agent is still attached to a "faecal deposit" after running the Detachment Sub-model and hence cannot move during the current timestep; 3) the FIO-agent is in the soil but does not exfiltrate when the Surface Routing Sub-model is run on the current timestep; 4) the FIO-agent remains in an area of degraded soil following the Seepage Sub-model being run on the current timestep; 5) the agent is deposited on the stream bed as it is routed through the channel by the Channel Routing Sub-model; or 6) the FIO-agent is successfully routed to the catchment outlet by the Channel Routing Sub-model (Figure 4b).

3.4 Design concepts

Of the 11 design concepts outlined in the ODD protocol, only basic principles, emergence, sensing, interaction, stochasticity and observation are relevant to MAFIO.

3.4.1 Basic principles

The process-based, spatially-distributed nature of MAFIO reflects the need for such models to further quantitative process understanding of water quality dynamics (de Brauwere et al., 2014) and to overcome limitations associated with lumped/semi-distributed model structures (Section 2.1). The principles underlying the process-based simulation of FIO loading, die-off and transport within MAFIO are as follows (Figure 1).

The Defecation Sub-model (Section 3.7.1) conceptualises FIO loading by livestock, assumed to be the main source of FIOs in agricultural areas (Chadwick et al., 2008). Loading by different livestock types can be simulated to account for differences in defecation characteristics (e.g. concentration of FIOs in faeces; Oliver et al., 2018) and FIO behaviour (e.g. die-off kinetics; Avery et al., 2004). FIO loading can be onto the land or directly into the channel via direct deposition (Chadwick et al., 2008). The potential for the latter depends on farm management, such as whether streams are fenced/gated off from the surrounding fields (Kay et al., 2007; Vinten et al., 2008). A sample of the FIOs loaded into the environment by individual animals is simulated in MAFIO by introducing one FIO-agent into the simulation for every specified number of FIOs loaded in reality (c.f. Parry and Bithell, 2012). This ensures that FIO-agents are introduced in correct proportions to account for different loadings by individual animals and livestock types. The accuracy with which the behaviour of the true population of FIOs can be inferred and resolved will vary with the number of FIOs for which an FIO-agent is introduced and the consequent total number of FIO-agents in the simulation (c.f. Parry and Bithell, 2012; Reaney, 2008).

386

387 The Die-off Sub-model (Section 3.7.2.1) conceptualises the die-off of FIOs in response to temperature
388 and solar radiation once in the environment; these factors are often considered the most important in
389 determining FIO mortality (Blaustein et al., 2013; Hipsey et al., 2008). Both are used to determine the
390 die-off of FIO-agents on the land surface, whilst only temperature is used for die-off of FIO-agents in
391 the soil (Whitehead et al., 2016). Given the likely short (<1 day) travel-times of water in small
392 agricultural streams, it is assumed that die-off of FIOs once in the stream is negligible. It may also be
393 possible for FIOs to grow in the environment (e.g. Muirhead, 2009; Soupir et al., 2008). However, given
394 the limited extent to which this process is understood and the consequent uncertainty (e.g. Hipsey et al.,
395 2008; Oliver et al., 2010), it is not considered in this initial development of MAFIO.

396

397 The Detachment Sub-model (Section 3.7.2.2) simulates the release of FIO-agents from faecal deposits
398 using a model based on effective precipitation depth and the assumption that this metric is sufficient to
399 allow observed release kinetics to be captured (Blaustein et al., 2015b). Once released, lateral transport
400 of FIOs can occur via overland flow, whilst infiltration may cause FIOs to move vertically into the soil
401 where soil retention effects including straining and filtering may limit their further transport (Oliver et
402 al., 2005a). Consequently, lateral movement of FIO-agents in MAFIO is only possible via overland
403 flow; infiltrating FIO-agents are retained in the soil. However, FIOs are generally retained in the upper
404 few centimetres of the soil, which may be within the "effective depth of interaction" of the soil with
405 surface flows that could facilitate lateral movement of the FIOs (Stocker et al., 2015). To account for
406 this, infiltrated FIO-agents can be exfiltrated back to the surface for transport in overland flow. These
407 processes of lateral movement, infiltration and exfiltration are conceptualised within the Surface
408 Routing Sub-model (Section 3.7.2.3).

409

410 In agricultural settings, compaction in areas of animal congregation or locations where there is a high
411 frequency of livestock traffic (e.g. gateways between fields) can cause soil degradation (Bilotta et al.,
412 2007). If proximal to the channel, this can increase the likelihood that these low permeability areas will
413 seep water and contaminants to the stream, potentially causing them to act as chronic sources of FIOs
414 (Davies-Colley et al., 2004). For cells containing a channel where degraded soil is present, the Seepage
415 Sub-model (Section 3.7.2.4) simulates this transfer to the stream.

416

417 Once in the stream, FIOs have an increased likelihood of settling to the channel bed if attached to
418 sediment (Pachepsky and Shelton, 2011). Several attempts have been made to model the settling of
419 sediment-associated FIOs (e.g. Collins and Rutherford, 2004; Hipsey et al., 2008; Jamieson et al., 2005;

Kim et al., 2010). However, substantial uncertainty still surrounds exactly how the process of settling should be represented (Pachepsky and Shelton, 2011; Pandey et al., 2012). Consequently, a simple distance-decay approach is initially adopted in MAFIO, with the likelihood of an FIO-agent settling to the streambed increasing with distance travelled within the stream. The exact form of the relationship can be assumed to implicitly account for different factors (e.g. settling velocity) affecting the likelihood of settling (Kay and McDonald, 1980). The association of FIO-agents with stream sediment and their resulting transport in the stream is simulated by the Channel Routing Sub-model (Section 3.7.2.5). Whilst resuspension of FIOs has been found to contribute to stream FIO dynamics (Pachepsky and Shelton, 2011), this is not currently included in MAFIO as in the relatively low-energy streams characteristic of small agricultural catchments, settling will be the dominant process except in the largest flow events (c.f. Nagels et al., 2002). Therefore, only settling was considered to assess whether this is sufficient to capture observed FIO dynamics (c.f. Clark et al., 2011).

3.4.2 Emergence

The model environments impose certain constraints on how simulations can unfold. For example, livestock counts, stream accessibility to livestock and locations of degraded soil determine into which land parcels FIO-agents can be spawned, where direct deposition may occur and where FIO-agents may chronically seep to the stream, respectively; thus, the field-scale distribution of *possible* FIO source areas is relatively imposed. Furthermore, the spatial distribution and magnitude of hydrological fluxes dictate where there are active flow paths capable of transporting FIO-agents. However, it is from simulating the small-scale behaviour of FIO-agents and their interaction with the variables of the model environments that the following simulated characteristics emerge: 1) The spatial distribution of FIO-agents stored on the surface and in the soil at the sub-field scale; 2) Fluxes of FIO-agents in the stream; 3) The pathways taken by FIO-agents from their source areas to the stream; 4) Time-varying contributions of FIO-agents to the stream made by different transfer mechanisms (overland flow, seepage and direct deposition) and host livestock; 5) The total number of FIO-agents active in the model domain at a given time.

3.4.3 Sensing and interaction

The behaviour of an FIO-agent is simulated based on it knowing its own attributes and those of the grid cell it currently occupies. Consequently, there are no interactions between FIO-agents, with all behaviours happening independently. A one-way interaction occurs between the FIO-agents and the spatial grid, with the FIO-agents responding to the conditions in the grid cell they occupy.

454 *3.4.4 Stochasticity*

455 MAFIO employs the following stochastic elements. In the Defecation Sub-model, uniform random
456 sampling (c.f. Dorner et al., 2006; Haydon and Deletic, 2006) determines the spatial grid cells into
457 which new FIO-agents are spawned to reflect natural variability (Benhamou, 2006, 2013) and
458 uncertainty in livestock movement and consequent defecation locations at the sub-field scale. If an FIO-
459 agent spawns in a cell containing a channel to which livestock have access, stochasticity is used to
460 ensure that direct deposition occurs with a frequency that reflects the size of the channel relative to the
461 total cell area. Whilst the number of FIOs shed by individual animals of different livestock types is
462 currently deterministic (i.e. relies on fixed parameters to specify factors such as FIO concentrations in
463 faeces, allowing MAFIO to be used in data-limited situations), variability and uncertainty in this
464 variable could be accounted for stochastically where a basis exists for defining reasonable sampling
465 distributions for relevant parameters (e.g. Schijven et al., 2015).

466

467 The Die-off, Detachment and Channel Routing Sub-models employ stochasticity to define the
468 behaviour of individual FIO-agents based on governing equations that describe population-level
469 behaviour. In the Surface Routing Sub-model, stochasticity conserves "concentrations" of FIO-agents
470 in hydrological stores (i.e. Ponded Surface Water and Soil Water) and fluxes (e.g. infiltration,
471 exfiltration). With the assumption that FIO-agents are fully and uniformly mixed within a hydrological
472 store, probabilities define the behaviour of individual FIO-agents such that when a hydrological flux is
473 generated, the proportion of water from the store that generates the flux is equal to the proportion of
474 FIO-agents in the store that it transports. Finally, the Seepage Sub-model employs stochasticity to
475 represent the general tendency for increased seepage potential as soils degrade in response to greater
476 livestock compaction and wetness, without explicitly representing poorly-defined seepage processes
477 (c.f. Collins and Rutherford, 2004).

478

479 *3.4.5 Observation*

480 For each timestep, the simulated flux of FIO-agents in the stream is recorded for each cell containing a
481 channel. This facilitates comparison with spatially-distributed observations of stream FIO loads. For
482 FIO-agents ultimately reaching the catchment outlet, the following attributes are observed: *Domain*
483 *type*, *Livestock type*, *Location memory* (Table 2). These observations are fundamental to MAFIO
484 fulfilling its stated purpose (Section 3.1) as they allow derivation of the transfer mechanisms, host
485 animals and pathways contributing FIOs to the stream at each timestep. The number and spatial
486 distribution of active FIO-agents in the model domain is also observed at each timestep so FIO-agent
487 fluxes can be linked to storage dynamics. Simulated outputs should be observed for an ensemble of

model runs using the same inputs and parameterisation to account for the effects of stochasticity in MAFIO (Abdou et al., 2012).

3.5 Initialisation

For the first timestep, an initial value of D_{frac} must be specified for each cell containing degraded soil to account for previous actions of livestock. Ideally, values should be based on livestock counts prior to the simulation start date; otherwise representative average counts (e.g. from the simulation period) may be used. In addition, each land parcel may be initialised with FIO-agents in the soil to allow for the possibility that FIOs from soil reservoirs reflecting past grazing patterns (which may persist for several months) contribute to FIO dynamics of the simulation period (Muirhead, 2009). Specifically, a number of FIO-agents can be randomly seeded in the soil of each land parcel at the start of the simulation based on estimates of FIOs in the soil derived from concentrations measured in the upper soil profiles of each land parcel, past livestock counts or literature values. Whilst initial values of D_{frac} and the number of FIO-agents to be seeded in the soil are consistent between simulations, the spatial locations of the latter are determined stochastically and therefore vary.

3.6 Inputs

MAFIO requires input data to characterise the catchment and hydrological environments. Table 3 documents those required for the catchment environment. The hydrological environment is characterised using inputs from an appropriate hydrological model, as detailed in Section 3.2.2. Spatially distributed inputs are provided as map files (.map) compatible with PCRaster (Karssenberg et al., 2010).

3.7 Sub-models

MAFIO consists of the Defecation Sub-model and several small-scale behaviour sub-models (Figure 4). The required parameters and their initial values based on daily simulation of *E. coli* from sheep and cattle are given in Table 4. In the following equations, a sub-script *[LS]* denotes that the value of the variable or parameter varies based on the livestock type. Meanwhile, a sub-script *[xy]* indicates an attribute or derived variable of the spatial grid whose value varies depending on the cell.

3.7.1 Defecation Sub-model

519 The Defecation Sub-model runs once every timestep (Figure 4a). The parameter *lsType* indicates which
520 livestock are being considered in the simulation. For each livestock type, the number of FIO-agents
521 introduced into the simulation for each defecation of an individual animal is calculated. First, the
522 concentration of FIOs per gram of faeces is specified by the parameter *faecesConc*. Total FIO loading
523 per defecation (*FIO_Load*) is then calculated as:

524

525 $$FIO\_Load_{[LS]} = faecesConc_{[LS]} * FWeight_{[LS]} \qquad Eq.5$$

526

527 where *FWeight* is the weight of a single defecation in grams. This value is then translated into a number
528 of FIO-agents introduced into the simulation per defecation (*LS_Agents*), based on a specified number
529 of FIOs assumed to be represented by an FIO-agent (*agentsRepresent*):

530

531 $$LS\_Agents_{[LS]} = \left\lceil \frac{FIO\_Load_{[LS]}}{agentsRepresent} \right\rceil \qquad Eq.6$$

532

533 For each livestock type, the Defecation Sub-model then introduces FIO-agents to land parcels based on
534 livestock counts for the current timestep. For each individual of a given livestock type, the number of
535 defecations per timestep is specified by *defecationsPerDay*. For each defecation, a cell of the current
536 land parcel is chosen using uniform random sampling. At this location, the number of FIO-agents
537 specified by *LS_Agents* are spawned. If the cell contains a channel (specified by $Chan_{Att}$ of the cell)
538 accessible to livestock, the probability that the FIO-agents spawn in the channel to simulate direct
539 deposition is:

540

541 $$P(Channel) = P\_Chan_{Att_{[xy]}} \qquad Eq.7$$

542

543 If they do not spawn in the channel or livestock do not have channel access, the FIO-agents either spawn
544 in an area of degraded soil if present (specified by $degSoil_{Att}$), or on the land adjacent to the channel.
545 Whilst the fixed nature of *faecesConc*, *FWeight*, and *defecationsPerDay* dictates that the number of
546 FIO-agents introduced by individual animals of a given livestock type is deterministic, as noted in
547 Section 3.4.4, stochastic treatment of this variable is possible if data exist to constrain appropriate
548 sampling distributions for the aforementioned parameters.

549

550 *3.7.2 Small-scale behaviour sub-models*

551 The small-scale behaviour sub-models simulating FIO-agent behaviour resulting from fate and transport
552 processes operating at the sub-field scale are applied every timestep to each FIO-agent in the model
553 domain in turn (Figure 4a). The exact sequence of sub-models that runs depends on certain attributes
554 of the FIO-agent in question (Figure 4b). MAFIO will move on to simulate the behaviour of the next
555 FIO-agent only once one of the six conditions in Section 3.3 are met.

556

557 *3.7.2.1 Die-off Sub-model*

558 The Die-off Sub-model (Figure 5) only runs for FIO-agents that spawned before the current timestep
559 (Figure 4b), with die-off modelled based on first-order kinetics following Chick's Law (Chick, 1908):

560

561 $$\frac{N_{Alive}}{N_0} = e^{-k_{dead} \cdot T} \qquad Eq. 8$$

562

563 where N_{Alive}/N_0 is the fraction of the original population of FIOs (N_0) that is still alive (N_{Alive}) after being
564 subject to exponential decay over a timestep, T, at a rate specified by the inactivation rate constant
565 parameter k_{dead} with units of T^{-1}. To translate this population-level behaviour to individual FIO-agents,
566 a probability that an FIO-agent dies is derived from Eq. 8 that is a function of the attributes of the grid
567 cell it occupies and its host animal:

568

569 $$P(Dies) = 1 - e^{-k_{dead_{[LS][xy]}} \cdot T} \qquad Eq. 9$$

570

571 Eq. 9 assumes all FIO-agents from a given livestock type within a cell can be treated as a single
572 population experiencing the same conditions and probability of die-off. The parameter k_{dead} is an overall
573 inactivation rate constant obtained by summing the individual inactivation rate constants arising from
574 factors (temperature and solar radiation in MAFIO) assumed to cause die-off (Chapra, 1997). The
575 inactivation rate constant due to temperature (k_{temp}) is based on the equation proposed by Mancini
576 (1978):

577

$$k_{temp_{[LS][xy]}} = k_{0_{[LS]}} . \theta_{[LS]}^{TS_{Att[xy]}-20} \quad Eq.10$$

where k_0 is the inactivation rate constant (units of T^{-1}) at a reference temperature of 20 °C, and θ is a temperature sensitivity parameter (dimensionless). Meanwhile, the inactivation rate constant due to solar radiation (k_{solar}) is calculated as (Thomann and Mueller, 1987):

$$k_{solar_{[LS][xy]}} = \alpha_{SR} . SR_{Att_{[xy]}} \quad Eq.11$$

where α_{SR} is a proportionality constant. When solar radiation is expressed in units of *ly* hr^{-1}, α_{SR} is approximately unity (Thomann and Mueller, 1987). The final value of k_{dead} depends on whether the FIO-agent is in the soil (Eq. 12a) or on the surface (Eq. 12b):

$$k_{dead_{[LS][xy]}} = k_{temp_{[LS][xy]}} \quad Eq.12a$$

$$k_{dead_{[LS][xy]}} = k_{temp_{[LS][xy]}} + k_{solar_{[LS][xy]}} \quad Eq.12b$$

If an FIO-agent dies, its attribute *Life state* is set to "0" so that it is no longer moved or tracked for the rest of the simulation.

3.7.2.2 Detachment Sub-model

The Detachment Sub-model (Figure 6) only runs for FIO-agents with the attribute *Detached-faeces* = "0" and *Life state* = "1" (Figure 4b). In MAFIO, the exponential model of Bicknell et al. (1997) simulates the rainfall-induced release of FIOs from faeces:

$$\frac{N_{Release}}{N_{Feaces}} = 1 - e^{-k_{release} . P} \quad Eq.13$$

where $N_{Release}/N_{Faeces}$ is the fraction of FIOs in the faeces (N_{Faeces}) released ($N_{Release}$), $k_{release}$ is a rate constant with units of cm^{-1} and P is precipitation (centimetres). This is used because it is a single-

parameter model that has not been shown to be substantially worse than alternative multi-parameter models (Blaustein et al., 2015a, 2016). From Eq. 13, the probability that an FIO-agent is detached from its faecal deposit is derived as:

$$P(Detached_{Faeces}) = 1 - e^{-k_{release} \cdot P_{Att[xy]}} \quad Eq.14$$

Despite the value of $k_{release}$ likely varying with livestock type (e.g. reflecting differently-composed faeces; c.f. Hodgson et al., 2009), a current lack of information (c.f. Sokolova et al., 2018) dictates this parameter be specified for the type of FIO being modelled. If the FIO-agent is detached, then *Detached-faeces* is set to "1" so that the Surface Routing Sub-model can run (Figures 4b and 6). Otherwise, the FIO-agent cannot move for the current timestep.

3.7.2.3 Surface Routing Sub-model

The Surface Routing Sub-model (Figure 7) only runs for FIO-agents with the attributes *Life state* = "1", *Detached-faeces* = "1" and *Domain type* = "Land" or "Land_Channel" (Figure 4b). The sub-model assumes full and immediate mixing of FIO-agents within hydrological stores and fluxes (c.f. Dorner et al., 2006); consequently, as soon as an FIO-agent enters a new hydrological store (i.e. Ponded Surface Water or Soil Water), it is immediately available for transport from that store in a hydrological flux (e.g. overland flow, exfiltration). The validity of this assumption varies with cell size, being more valid for smaller grid cells (Reaney, 2008).

For each timestep, the Surface Routing Sub-model proceeds as follows for each applicable FIO-agent (Figure 7). If the attribute *Infiltration stage* of the FIO-agent is not equal to "Soil", its infiltration into the soil is determined based on a probability of infiltration:

$$P(Infiltrate) = P\_Infil_{Att_{[xy]}} \quad Eq.15$$

If the FIO-agent infiltrates, its attribute *Infiltration stage* is set to "Soil". Whether it exfiltrates back to the surface then depends on a probability of exfiltration:

$$P(Exfiltrate) = P\_Exfil_{Att_{[xy]}} \quad Eq.16$$

If the *Infiltration stage* attribute of the FIO-agent was already "Soil" to begin with, only the potential for exfiltration is evaluated. If the FIO-agent exfiltrates, its *Infiltration stage* attribute is set to "Surface". If after infiltration and exfiltration the FIO-agent has *Infiltration stage* equal to "Surface", then it is assumed to be transported laterally in overland flow, and its attribute *Movement tracker* is set to "1". If the FIO-agent is already in a cell containing a channel (cell with $Chan_{Att}$ = 1), then its attribute *Domain type* is set to "Channel" to denote that overland flow has transported the FIO-agent from the land adjacent to the channel into the channel itself; the sub-model then exits and the Channel Routing Sub-model runs (Figure 4b). If not already in a cell with *ChanAtt* = 1, the FIO-agent moves to the downslope cell based on $fDir_{Att}$ of the cell it currently occupies. If the FIO-agent moves into a cell with $Chan_{Att}$ =1, what happens next depends on the presence of degraded soil (specified by $degSoil_{Att}$). If present, the *Domain type* and *Infiltration stage* attributes of the FIO-agent are changed to "Seepage" and "Soil", respectively, and the sub-model exits so the Seepage Sub-model can run (Figure 4b). If not present, then *Domain type* is set to "Land_Channel" and the Surface Routing Sub-model runs again to determine whether the FIO-agent infiltrates into the soil next to the channel or is routed into the channel. If the latter, *Domain type* is set to "Channel" and the sub-model exits so the Channel Routing Sub-model can run; otherwise MAFIO moves on to simulate the next FIO-agent (Figure 4b). If the FIO-agent did not move into a cell with $Chan_{Att}$ = 1, the Surface Routing Sub-model continues until the FIO-agent infiltrates into the soil but does not exfiltrate, reaches an area of degraded soil or enters the channel; an FIO-agent cannot, therefore, remain on the surface after the Surface Routing Sub-model has run.

3.7.2.4 Seepage Sub-model

The Seepage Sub-model (Figure 8) runs for FIO-agents with *Life state* and *Domain type* = "1" and "Seepage", respectively (Figure 4b). It determines whether an FIO-agent in an area of degraded soil adjacent to the channel seeps to the stream based on a probability of seepage:

$$P(Seep) = P\_Seep_{Att_{[xy]}} \quad Eq.17$$

If the FIO-agent seeps to the stream, its attribute *Domain type* is set to "Channel" so the Channel Routing Sub-model can run (Figure 4b). Otherwise, the FIO-agent remains in the degraded soil for the current timestep. Whilst the Seepage Sub-model does not utilise any parameters, it is necessary to

specify the number of livestock units each animal of a given livestock type represents (*LUs*), the values of livestock units per hectare that constitute the "low", "medium" and "high" risk bands (*riskBands*), the damage fraction associated with each risk band (*dFrac_Bands*) and the rate constant for the exponential decline in damage fraction over time (k_d) used in the calculation of the spatial grid attribute P_Seep_{Att}, (Section 3.2.4).

3.7.2.5 Channel Routing Sub-model

The Channel Routing Sub-model (Figure 9) runs for FIO-agents with *Domain type* = "Channel" (Figure 4b). First, the sub-model determines whether the FIO-agent attaches to stream sediment when entering the channel based on the parameter *fracAttached*:

$$P(Attached_{StreamSed}) = fracAttached \qquad Eq.18$$

If the FIO-agent does not attach, it is assumed it cannot settle to the streambed and the FIO-agent is routed through the channel network to the catchment outlet. If the FIO-agent attaches, its attribute *Attached-stream sediment* is set to "1", and routing occurs as follows. The probability that the FIO-agent settles to the streambed in its current cell is determined based on length of the channel in the cell (*streamDist*) and the distance-decay model of Kay and McDonald (1980):

$$P(Settle) = 1 - 10^{-\lambda_{sed}.streamDist_{[xy]}} \qquad Eq.19$$

where λ_{sed} is the rate constant parameter in units of m^{-1}. If the FIO-agent does not settle, it is routed to the next downstream cell, and the probability is calculated again. This continues until the FIO-agent settles to the streambed or is routed out of the catchment. Once the FIO-agent reaches the cell representing the catchment outlet, it may still settle to account for the length of the stream in that cell. As with the Surface Routing Sub-model, the Channel Routing Sub-model assumes full and immediate mixing of FIO-agents within each cell. In addition, it assumes that all FIO-agents passing through a cell can be considered as a single population experiencing the same decay with distance, similar to the Die-off Sub-model.

4 A hydrological environment generator: *EcH$_2$O-iso*

4.1 Overview of EcH_2O-iso

EcH_2O-iso is a process-based, spatially-distributed ecohydrological model that simulates coupled energy, hydrological and vegetation dynamics (Kuppel et al., 2018b; Maneta and Silverman, 2013) with the capacity to track the stable isotope (^2H and ^{18}O) compositions and water ages of simulated hydrological stores and fluxes (Kuppel et al., 2018a). EcH_2O-iso has successfully been applied to temperate (Kuppel et al., 2018a) and cold (Smith et al., 2019) regions, and at the plot- (Douinot et al., 2019) to catchment-scale (Knighton et al., 2020; Kuppel et al., 2018a; Smith et al., 2019), demonstrating the versatility of the model in different environments and process domains.

EcH_2O-iso has assumed full and immediate mixing for tracer and age tracking within each liquid hydrological store to minimize parameterization and computing time (Kuppel et al., 2018a). However, limitations to this approach have been highlighted, even in wet, energy-limited catchments where heterogeneous mixing and flow is reduced compared to other ecoclimatic settings (Geris et al., 2015; Kuppel et al., 2018a). More generally, there is a need to consider partial mixing in tracer-aided models (Cain et al., 2019; Knighton et al., 2017) to accommodate possible ecohydrological separation of water in the subsurface – that is its partitioning between water that is tightly-bound to the soil matrix in small pores and mobile water which may predominantly contribute to groundwater recharge and streamflow (Brooks et al., 2010; Goldsmith et al., 2012; Sprenger et al., 2018). To the authors' knowledge, two-pore conceptualisations of the subsurface in physically-based models are only just emerging in catchment studies (Hopp et al., 2020), with efforts largely having been limited to the plot scale (Jackish and Zehe, 2018; Sprenger et al., 2018; Stumpp and Maloszewski, 2010; Vogel et al., 2010).

To incorporate heterogeneous subsurface mixing, EcH_2O-iso has been updated so that the tracked isotopic composition and age of water considers a two-pore domain in the upper two layers of the three-layer soil profile (Figure 10). The two domains (tightly-bound [TB] and mobile [MW]) are distinguished using a tension threshold for mobile water (Ψ_{MW}), a parameter shared by both layers, with a corresponding water content threshold (SWC_{MW}) determined by the Brooks-Corey pedo-transfer functions used in EcH_2O-iso (Maneta and Silverman, 2013). In each layer, the MW domain only exists if total water storage in the layer (SWC_t) exceeds the storage capacity of TB ($SWC_t > SWC_{\mathrm{MW}}$). Liquid water fluxes downwards (infiltration and percolation) and upwards (return flow) draw from MW and primarily refill TB, except for surface water considered as MW (Figure 10). Secondary flow paths (MW to MW) occur if the recipient TB reaches its maximum storage capacity. Soil evaporation and plant transpiration draw from both domains in proportion to their respective water contents. After evaporative losses, dispersion replenishes TB from MW (potentially emptying MW), assuming continuity in water contents between the two domains.

The two-pore domain conceptualisation only affects tracer and age tracking; computation of water fluxes between layers (infiltration/percolation, return flow) and from the subsurface system (soil evaporation, transpiration) is unchanged from previous versions of EcH_2O-iso. The groundwater store is also still defined using a field capacity tension threshold (Ψ_{FC}, fixed to 3.36 m), and tracking assumes full mixing within the 3rd soil layer even if unsaturated (Figure 10). The remaining workings of EcH_2O-iso are as described in Maneta and Silverman (2013) and Kuppel et al. (2018a, b), with the further addition of species-dependent root profiles as implemented in Douinot et al. (2019) and Knighton et al. (2020).

4.2 Interfacing EcH_2O-iso with MAFIO

EcH_2O-iso provides all outputs required to characterise the hydrological environment of MAFIO. However, EcH_2O-iso simulates infiltration twice within a grid cell, first following the addition of effective precipitation to ponded surface water and then again after the addition of snowmelt and run-on from upslope cells (see Figure 1 in Kuppel et al., 2018a). For processes in MAFIO to be consistent with this, two probabilities of infiltration need to be assigned to each cell of the spatial grid (P_Infil1_{Att} and P_Infil2_{Att}). Then, FIO-agents which have been detached by rainfall on a given timestep and are still in their initial cell may first infiltrate with probability P_Infil1_{Att} and then, if still on the surface, with probability P_Infil2_{Att}, whilst FIO-agents which move into a cell in run-on from upslope can only infiltrate with probability P_Infil2_{Att}. This aside, the process conceptualisation of EcH_2O-iso is compatible with the catchment conceptualisation represented by the variables of the hydrological environment of MAFIO (Section 3.2.2). As EcH_2O-iso conceptualises three hydrological layers in the soil, *Exfil*, SWC_{Exf} and Sat_{Def} are taken from the upper layer to be consistent with the representation of the upper soil profile in MAFIO.

5 Conclusions

This paper has reported the rationale for and development of MAFIO, a new agent-based model for simulating the behaviour and transport of agents representing FIOs. The model is intended to elucidate the sources and transfer mechanisms contributing FIOs to streams at the sub-field scale in small agricultural catchments, with improved confidence in hydrological process representation afforded by the use of a robust external model for simulating the hydrological environment. Here, the spatially-distributed, tracer-aided ecohydrological model EcH_2O-iso was introduced as an exemplar hydrological environment generator. A companion paper (Neill et al., *in review*) provides a proof-of-concept

application of MAFIO focusing on process representation and the potential the model has for use in a management context.

Software availability

The source code for MAFIO as outlined in this work is available via the University of Aberdeen PURE repository: *https://doi.org/10.20392/66f74663-ece3-4a52-8bed-f0cf52d0831a*

The source code for EcH$_2$O-iso is available at: https://bitbucket.org/sylka/ech2o_iso/src/master_2.0/

Acknowledgements

Funding for this work from the Scottish Government's Hydro Nation Scholars Programme is gratefully acknowledged. Many thanks go to Sim Reaney and John Wainwright for initial discussions regarding environmental agent-based modelling approaches and methods for their implementation.

References

Abdou, M., Hamill, L., Gilbert, N., 2012. Designing and Building an Agent-Based Model: 141-166 in Heppenstall, A.J., Crooks, A.T., See, L.M., Batty, M. (eds). Agent-Based Models of Geographical Systems. Springer: Dordrecht, Heidelberg, London, New York.

Ala-aho, P., Tetzlaff, D., McNamara, J.P., Laudon, H., Soulsby, C., 2017. Using isotopes to constrain water flux and age estimates in snow-influenced catchments using the STARR (Spatially distributed Tracer-Aided Rainfall-Runoff) model. Hydrological Earth Systems Science 21: 5089-5110.

Avery, S.M., Moore, A., Hutchison, M.L., 2004. Fate of *Escherichia coli* originating from livestock faeces deposited directly onto pasture. Letters in Applied Microbiology 38: 355-359.

Benhamou, S., 2006. Detecting an orientation component in animal paths when the preferred direction is individual-dependent. Ecology 87: 518-528.

Benhamou, S., 2013. Of scales and stationarity in animal movements. Ecology Letters 17: 261-272.

Berman, E.S.F., Levin, N.E., Landais, A., Li, S., Owano, T., 2013. Measurement of $\delta^{18}O$, $\delta^{17}O$, and ^{17}O-excess in Water by Off-Axis Integrated Cavity Output Spectroscopy and Isotope Ratio Mass Spectrometry. Analytical Chemistry 85: 10392-10398.

Bicknell, B.R., Imhoff, J.C., Kittle Jr., J.L., Donigan Jr., A.S., Johanson, R.C., 1997. Hydrological simulation program – FORTRAN user's manual for version 11. Environmental Protection Agency Report No: EPA/600/R-97/080. U.S. Environmental Protection Agency: Athens, Ga.

Bilotta, G.S., Brazier, R.E., Haygarth, P.M., 2007. The impacts of grazing animals on the quality of soils, vegetation and surface waters in intensively managed grasslands. Advances in Agronomy 94: 237-280.

Birkel, C., Soulsby, C., 2015. Advancing tracer-aided rainfall-runoff modelling: a review of progress, problems and unrealised potential. Hydrological Processes 29: 5227-5240.

Birkel, C., Soulsby, C., Tetzlaff, D., 2014a. Developing a consistent process-based conceptualization of catchment functioning using measurements of internal state variables. Water Resources Research 50: 3481-3501.

Birkel, C., Soulsby, C., Tetzlaff., D. 2014b. Integrating parsimonious models of hydrological connectivity and soil biogeochemistry to simulate stream DOC dynamics. Journal of Geophysical Research 119: 1030-1047.

Blaustein, R.A., Hill, R.L., Micallef, S.A., Shelton, D.R., Pachepsky, Y.A., 2016. Rainfall intensity effects on removal of fecal indicator bacteria from solid dairy manure applied over grass-covered soil. Science of the Total Environment 539: 583-591.

Blaustein, R.A., Pachepsky, Y., Hill, R.L., Shelton, D.R., 2015a. Solid manure as a source of fecal indicator microorganisms: Release under simulated rainfall. Environmental Science and Technology 49: 7860-7869.

Blaustein, R.A., Pachepsky, Y., Shelton, D.R., Hill, R.L., 2015b. Release and removal of microorganisms from land-deposited animal waste and animal manures: A review of data and models. Journal of Environmental Quality 44: 1338-1354.

Blaustein, R.A., Pachepsky, Y., Hill, R.L., Shelton, D.R., Whelan, G., 2013. *Escherichia coli* survival in waters: Temperature dependence. Water Research 47(2): 569-578

Brooks, J.R., Barnard, H.R., Coulombe, R., McDonnell, J.J., 2010. Ecohydrologic separation of water between trees and streams in a Mediterranean climate. Nature Geoscience 3: 100-104.

Brooks, P.D., Chorover, J., Fan, Y., Godsey, S.E., Maxwell, R.M., McNamara, J.P., Tague, C., 2015. Hydrological partitioning in the critical zone: Recent advances and opportunities for developing transferable understanding of water cycle dynamics. Water Resources Research 51: 6973-6987.

Cain, M.R., Ward., A.S., Hrachowitz, M., 2019. Ecohydrologic separation alters interpreted hydrologic stores and fluxes in a headwater mountain catchment. Hydrological Processes 33: 2658-2675.

Chadwick D., Fish, R., Oliver, D.M., Heathwaite, L., Hodgson, C., Winter, M., 2008. Management of livestock and their manure to reduce the risk of microbial transfers to water – the case for an interdisciplinary approach. Trends in Food Science and Technology 19: 240-247.

Chapra, S.C., 1997. Surface water-quality modelling. McGraw-Hill: New York.

Chick, H., 1908. Investigation of the laws of disinfection. Journal of Hygiene 8: 655.

Cho, K.H., Pachepsky, Y.A., Oliver, D.M., Muirhead, R.W., Park, Y., Quilliam, R.S., Shelton, D.R., 2016. Modeling fate and transport of fecally-derived microorganisms at the watershed scale: State of the science and future opportunities. Water Research 100: 38-56.

Cirbus, J., Podhoranyi, M., 2013. Cellular automata for the flow simulations on the Earth surface, optimisation computation process. Applied Mathematics and Information Sciences 7: 2149-2158.

Clark, M.P., Kavetski, D., Fenicia, F., 2011. Pursuing the method of multiple working hypotheses for hydrological modeling. Water Resources Research 47: W09301.

Collins, R., Rutherford, K., 2004. Modelling bacterial water quality in streams draining pastoral land. Water Research 38: 700-712.

Cooper, J.R., Wainwright, J., Parsons, A.J., Onda, Y., Fukuwara, T., Obana, E., Kitchener, B., Long, E.J., Hargrave, G.H., 2012. A new approach for simulating the redistribution of soil particles by water erosion: A marker-in-cell model. Journal of Geophysical Research 117: F04027.

Crooks, A.T., Heppenstall, A.J., Introduction to Agent-Based Modelling: 85-108 in Heppenstall, A.J., Crooks, A.T., See, L.M., Batty, M. (eds). Agent-Based Models of Geographical Systems. Springer: Dordrecht, Heidelberg, London, New York.

Davies-Colley, R.J., Nagels, J.W., Smith, R.A., Young, R.G., Phillips, C.J., 2004. Water quality impact of a dairy cowherd crossing a stream. New Zealand Journal of Marine and Freshwater Research 38(4): 569–576.

de Brauwere, A., Ouattara, N.K., Servais, P., 2014. Modeling fecal indicator bacteria concentrations in natural surface waters: A review. Critical Reviews in Environmental Science and Technology 44: 2380-2453.

Dick, J.J., Tetzlaff, D., Birkel, C., Soulsby, C., 2015. Modelling landscape controls on dissolved organic carbon sources and fluxes to streams. Biogeochemistry 122: 361-374.

Dorner, S.M., Anderson, W.B., Slawson, R.M., Kouwen, N., Huck, P.M., 2006. Hydrologic modeling of pathogen fate and transport. Environmental Science and Technology 40: 4746-4753.

Drewry, J.J., 2006. Natural recovery of soil physical properties from treading damage of pastoral soils in New Zealand and Australia: A review. Agriculture, Ecosystems and Environment 144: 159-169.

Douinot, A., Tetzlaff, D., Maneta, M., Kuppel, S., Schulte-Bisping, H., Soulsby, C., 2019. Ecohydrological modelling with EcH2O-iso to quantify forest and grassland effects of water partitioning and flux ages. Hydrological Processes 33: 2174-2191.

Elliot, A.H., Tian, Y.Q., Rutherford, J.C., Carlson, W.T., 2002. Effect of cattle treading on interrill erosion from hill pasture: modelling concepts and analysis of rainfall simulator data. Australian Journal of Soil Research 40: 963-976.

Falkenmark, M., Rockström, J., 2006. The new blue and green water paradigm: Breaking new ground for water resources planning and management. Journal of Water Resources Planning and Management 132: 129-132.

Fatichi, S., Vivoni, E.R., Ogden, F.L., Ivanov, V.Y., Mirus, B., Gochis, D., Downer, C.W., Camporese, M., Davison, J.H., Ebel, B., Jones, N., Kim, J., Mascaro, G., Niswonger, R., Restrepo, P., Rigon, R., Shen, C., Sulis, M., Tarboton, D., 2016. An overview of current applications, challenges, and future trends in distributed process-based models in hydrology. Journal of Hydrology 537: 45-60.

Fewtrell, L., Kay, D. 2015. Recreational water and infection: a review of recent findings. Current Environmental Health Reports 2(1): 85-94.

Geldreich, E.E., 1996. Pathogenic agents in freshwater resources. Hydrological Processes 10: 315-333.

Geris, J., Tetzlaff, D., McDonnell, J., Anderson, J., Paton, G., and Soulsby, C., 2015. Ecohydrological separation in wet, low energy northern environments? A preliminary assessment using different soil water extraction techniques. Hydrological Processes 29: 5139-5152.

Goldsmith, G.R., Munoz-Villers, L.E., Holwerda, F., McDonnell, J.J., Asbjornsen, H., Dawson, T.E., 2012. Stable isotopes reveal linkages among ecohydrological processes in a seasonally dry tropical montane cloud forest. Ecohydrology 5: 779-790.

Greene, S., Johnes, P.J., Bloomfield, J.P., Reaney, S.M., Lawley, R., Elkhatib, Y., Freer, J., Odoni, N., Macleod, C.J.A., Percy, B., 2015. A geospatial framework to support integrated biogeochemical modelling in the United Kingdom. Environmental Modelling and Software 68: 219-232.

879 Grimm, V., Berger, U., DeAngelis, D.L., Polhill, J.G., Giske, J., Railsback, S.F., 2010. The ODD protocol: A
880 review and first update. Ecological Modelling 221: 2760-2768.

881 Grimm, V., Berger, U., Bastiansen, F., Eliassen, S., Ginot, V., Giske, J., Goss-Custard, J., Grand, T., Heinz, S.K.,
882 Huse, G., Huth, A., Jepsen, J.U., Jørgensen, C., Mooij, W.M., Müller, B., Pe'er, G., Piou, C., Railsback,
883 S.F., Robbins, A.M., Robbins, M.M., Rossmanith, E., Rüger, N., Strand, E., Souissi, S., Stillman, R.A.,
884 Vabø, R., Visser, U., DeAngelis, D.L., 2006. A standard protocol for describing individual and agent-
885 based models. Ecological Modelling 198: 115-126.

886 Haydon, S., Deletic, A., 2006. Development of a coupled pathogen-hydrologic catchment model. Journal of
887 Hydrology 328: 467-480.

888 Himathongkham, S., Bahari, S., Riemann, H., Cliver, D., 1999. Survival of *Escherichia coli* O157:H7 and
889 Salmonella typhimurium in cow manure and cow manure slurry. FEMS Microbiology Letters 178: 251-
890 257.

891 Hipsey, M.R., Antenucci, J.P., Brookes, J.D., 2008. A generic, process-based model of microbial pollution in
892 aquatic systems. Water Resources Research 44: W07408.

893 Hodge, R.A., Hoey, T.B., 2012. Upscaling from grain-scale processes to alluviation in bedrock channels using a
894 cellular automaton model. Journal of Geophysical Research 117: F01017.

895 Hodgson, C.J., Bulmer, N., Chadwick, D.R., Oliver, D.M., Heathwaite, A.L., Fish, R.D., Winter, M., 2009.
896 Establishing relative release kinetics of faecal indicator organisms from different faecal matrices. Letters
897 in Applied Microbiology 49: 124-130.

898 Hopp, L., Glaser, B., Klaus, J., & Schramm, T., 2020. The relevance of preferential flow in catchment scale
899 simulations: Calibrating a 3D dual-permeability model using DREAM. Hydrological Processes 34(5):
900 1237-1254.

901 Jackisch, C., Zehe, E., 2018. Ecohydrological particle model based on representative domains. Hydrology and
902 Earth Systems Science 22: 3639-3662.

903 Jamieson, R., Joy, D.M., Lee, H., Kostaschuk, R., Gordon, R., 2005. Transport and deposition of sediment-
904 associated *Escherichia coli* in natural streams. Water Research 39: 2665-2675.

905 Karr, J.R., Schlosser, I.J., 1978. Water resources and the land-surface interface. Science 201: 229-234.

906 Karssenberg, D., Schmitz, O., Salamon, P., de Jong, K., Bierkens, M.F.P., 2010. A software framework for
907 construction of process-based stochastic spatio-temporal models and data assimilation. Environmental
908 Modelling and Software 25: 489–502.

909 Kay, D., McDonald, A., 1980. Reduction of coliform bacteria in two upland reservoirs: The significance of
910 distance decay relationships. Water Research 14: 305-318.

Kay, D., Crowther, J., Stapleton, C.M., Wyer, M.D., Fewtrell, L., Anthony, S., Bradford, M., Edwards, A., Francis, C.A., Hopkins, M., Kay, C., McDonald, A.T., Watkins, J., Wilkinson, J., 2008. Faecal indicator organism concentrations and catchment export coefficients in the UK. Water Research 42: 2649-2661.

Kay, D., Aitken, M., Crowther, J., Dickson, I., Edwards, A.C., Francis, C., Hopkins, M., Jeffrey, W., Kay, C., McDonald, A.T., McDonald, D., Stapleton, C.M., Watkins, J., Wilkinson, J., Wyer, M.D., 2007. Reducing fluxes of faecal indicator compliance parameters to bathing waters from diffuse agricultural sources: The Brighouse Bay study, Scotland. Environmental Pollution 147: 138-149.

Kim, J., Pachepsky, Y.A., Shelton, D.R., Coppock, C., 2010. Effect of streambed bacteria release on *E. coli* concentrations: Monitoring and modeling with the modified SWAT. Ecological Modelling 221: 1592-1604.

Knighton, J., Saia, S.M., Morris, C.K., Archibald, J.A., Todd Walter, M., 2017. Ecohydrological considerations for modeling of stable water isotopes in a small intermittent watershed. Hydrological Processes 31: 2438-2452.

Knighton, J., Kuppel, S., Smith, A., Spenger, M., Soulsby, C., Tetzlaff, D., 2020. Using isotopes to incorporate tree water storage and mixing dynamics into a distributed hydrologic modeling framework. Ecohydrology 13: e2201.

Kuppel, S., Tetzlaff, D., Maneta, M.P., Soulsby, C., 2018a. EcH2O-iso 1.0: water isotopes and age tracking in a process-based, distributed ecohydrological model. Geoscientific Model Development 11: 3045-3069.

Kuppel, S., Tetzlaff, D., Maneta, M.P., Soulsby, C., 2018b. What can we learn from multi-criteria calibration of a process-based ecohydrological model? Environmental Modelling and Software 101: 301-316.

Macal, C.M., North, M.J., 2010. Tutorial on agent-based modelling and simulation. Journal of Simulation 4(3): 151-162.

Mancini, J.L., 1978. Numerical estimates of coliform mortality rates under various conditions. Journal of Water Pollution Control Federation 50: 2477-2484.

Maneta, M.P., Silverman, N.L., 2013 A spatially distributed model to simulate water, energy, and vegetation dynamics using information from regional climate models. Earth Interactions 17: 1–44.

McDonnell, J.J., Beven, K., 2014. Debates – The future of hydrological sciences: A (common) path forward? A call to action aimed at understanding velocities, celerities and residence time distributions of the headwater hydrograph. Water Resources Research 50: 5342-5350.

McKergow, L.A., Davies-Colley, R.J., 2010. Stormflow dynamics and loads of *Escherichia coli* in a large mixed land use catchment. Hydrological Processes 24: 276-289.

Moriarty, E.M., Mackenzie, M.L., Karki, N., Sinton, L.W., 2011. Survival of Escherichia coli, enterococci and Campylobacter spp. in sheep feces on pastures. Applied and Environmental Microbiology 77: 1797-1803.

945 Muirhead, R., 2009. Soil and faecal material reservoirs of *Escherichia coli* in a grazed pasture. New Zealand
946 Journal of Agricultural Research 52: 1-8.

947 Nagels, J.W., Davies-Colley, R.J., Donnison, A.M., Muirhead, R.W., 2002. Faecal contamination over flood
948 events in a pastoral agricultural stream in New Zealand. Water Science and Technology 45: 45-52.

949 Natural England, 2013. Higher level stewardship: Environmental stewardship handbook (Fourth Edition).
950 Available at: http://publications.naturalengland.org.uk/file/2819648

951 Neill, A.J., Tetzlaff, D., Strachan, N.J.C., Soulsby, C., 2019. To what extent does hydrological connectivity control
952 dynamics of faecal indicator organisms in streams? Initial hypothesis testing using a tracer-aided model.
953 Journal of Hydrology 570: 423-435.

954 Neill, A.J., Tetzlaff, D., Strachan, N.J.C., Hough, R.L., Avery, L.M., Maneta, M.P., Soulsby, C., *in review*. An
955 agent-based model that simulates the spatio-temporal dynamics of sources and transfer mechanisms
956 contributing faecal indicator organisms to streams. Part 2: Application to a small agricultural catchment.
957 Journal of Environmental Management.

958 O'Callaghan, J.F., Mark, D.A., 1984. The extraction of drainage networks from digital elevation data. Computer
959 Vision, Graphics and Image Processing 28: 323-344.

960 O'Sullivan, D., Millington, J., Perry, G. & Wainwright, J., 2012. Agent-based models – because they're worth it?:
961 109-123 in Heppenstall, A.J., Crooks, A.T., See, L.M., Batty, M. (eds). Agent-Based Models of
962 Geographical Systems. Springer: Dordrecht, Heidelberg, London, New York.

963 Oliver D.M., Clegg C.D., Haygarth P.M., Heathwaite A.L., 2005a. Assessing the potential for pathogen transfer
964 from grassland soils to surface waters. Advances in Agronomy 85: 125–180.

965 Oliver, D.M., Heathwaite, L., Haygarth, P.M., Clegg, C.D., 2005b. Transfer of Escherichia coli to Water from
966 Drained and Undrained Grassland after Grazing. Journal of Environmental Quality 34: 918-925.

967 Oliver, D.M., Heathwaite, A.L., Hodgson, C.J., Chadwick, D.R., 2007. Mitigation and current management
968 attempts to limit pathogen survival and movement within farmed grassland. Advances in Agronomy 93:
969 95-152.

970 Oliver, D.M., Page, T., Heathwaite, A.L., Haygarth, P.M., 2010. Re-shaping models of *E. coli* population
971 dynamics in livestock faeces: Increased bacterial risk to humans? Environmental International 36: 1-7.

972 Oliver, D.M., Bartie, P.J., Heathwaite, A.L., Reaney, S.M., Parnell, J.A.P., Quilliam, R.S., 2018. A catchment-
973 scale model to predict spatial and temporal burden of *E. coli* on pasture from grazing livestock. Science
974 of the Total Environment 616-617: 678-687.

975 Oliver, D.M., Fish, R.D., Hodgson, C.J., Heathwaite, A.L., Chadwick, D.R., Winter, M., 2009. A cross-
976 disciplinary toolkit to assess the risk of faecal indicator loss from grassland farm systems to surface
977 waters. Agriculture, Ecosystems and Environment 129: 401-412.

978 Oliver, D.M., Porter, K.D.H., Pachepsky, Y.A., Muirhead, R.W., Reaney, S.M., Coffey, R., Kay, D., Milledge,
979 D.G., Hong, E., Anthony, S.G., Page, T., Bloodworth, J.W., Mellander, P., Carbonneau, P., McGrane,
980 S.J., Quilliam, R.S., 2016. Predicting microbial water quality with models: Over-arching questions for
981 managing risk in agricultural catchments. Science of the Total Environment 544: 39-47.

982 Pachepsky, Y.A., Shelton, D.R., 2011. *Escherichia coli* and fecal coliforms in freshwater and estuarine sediments.
983 Critical Reviews in Environmental Science and Technology 41(12): 1067-1110.

984 Pandey, P.K., Soupir, M.L., Rehmann, C.R., 2012. A model for predicting resuspension of *Escherichia coli* from
985 streambed sediments. Water Research 46: 115-126.

986 Parry, H.R., Bithell, M., 2012. Large scale agent-based modelling: A review and guidelines for model scaling:
987 271-308 in Heppenstall, A.J., Crooks, A.T., See, L.M., Batty, M. (eds). Agent-Based Models of
988 Geographical Systems. Springer: Dordrecht, Heidelberg, London, New York.

989 Piovano, T.I., Tetzlaff, D., Ala-aho, P., Buttle, J., Mitchell, C.P.J., Soulsby, C., 2018. Testing a spatially
990 distributed tracer-aided runoff model in a snow-influenced catchment: Effects of multicriteria calibration
991 on streamwater ages. Hydrological Processes 30: 3089-3107.

992 Piovano, T.I., Tetzlaff, D., Carey, S.K., Shatilla, N.J., Smith, A., Soulsby, C., 2019. Spatially distributed tracer-
993 aided runoff modelling dynamics of storage and water ages in a permafrost-influenced catchment.
994 Hydrology and Earth Systems Science 23: 2507-2523.

995 Ravazzani, G., Rametta, D., Mancini, M., 2011. Macroscopic cellular automata for groundwater modelling: A
996 first approach. Environmental Modelling and Software 26: 634-643.

997 Reaney, S.M., 2008. The use of agent based modelling techniques in hydrology: determining the spatial and
998 temporal origin of channel flow in semi-arid catchments. Earth Surface Processes and Landforms 33:
999 317-327.

1000 Remondi, F., Kirchner, J.W., Burlando, P., Fatichi, S., 2018. Water flux tracking with a distributed hydrological
1001 model to quantify controls on spatio-temporal variability of transit time distributions. Water Resources
1002 Research 54: 3081-3099.

1003 Rode, M., Arhonditsis, G., Balin, D., Kebede, T., Krysanova, V., van Griensven, A., van der Zee, S.E.A.T.M.,
1004 2010. New challenges in integrated water quality modelling. Hydrological Processes 24: 3447-3461.

1005 Sadeghi, A., Arnold, J., 2002. A SWAT/Microbial Sub-Model for Predicting Pathogen Loadings in Surface and
1006 Groundwater at Watershed and Basin Scales. In Total Maximum Daily Load (TMDL): Environmental
1007 Regulations, Proceedings of 2002 Conference (p. 56). American Society of Agricultural and Biological
1008 Engineers.

1009 Schijven, J., Derx, J., de Roda Husman, A.M., Blaschke, A.P., Farnleitner, A.H., 2015. QMRAcatch: Microbial
1010 Quality Simulation of Water Resources including Infection Risk Assessment. Journal of Environmental
1011 Quality 44: 1491-1502.

Shao, Q., Weatherly, D., Huang, L., Baumgartl, T., 2015. RunCA: A cellular automata model for simulating surface runoff at different scales. Journal of Hydrology 529: 816-829.

Sheath, G.W., Carlson, W.T., 1998. Impact of cattle treading on hill land: 1. Soil damage patterns and pasture status. New Zealand Journal of Agricultural Research 41(2): 271-278.

Smith, A.A., Tetzlaff, D., Laudon, H., Maneta, M., and Soulsby, C., 2019. Assessing the influence of soil freeze-thaw cycles on catchment water storage-flux-age interactions using a tracer-aided ecohydrological model. Hydrology and Earth Systems Science 23: 3319-3334.

Sokolova, E., Lindström, G., Pers, C., Strömqvist, J., Lewerin, S.S., Wahlström, H., Sörén, K., 2018. Water quality modelling: microbial risks associated with manure on pasture and arable land. Journal of Water and Health 16(4): 549-561.

Soupir, M.L., Mostaghimi, S., Lou, J., 2008. Die-off of *E. coli* and Enterococci in dairy cowpats. Transactions of the ASABE 51(6): 1987-1996.

Sprenger, M., Tetzlaff, D., Buttle, J., Laudon, H., Leistert, H., Mitchell, C.P.J., Snelgrove, J., Weiler, M., Soulsby, C., 2018. Measuring and modeling stable isotopes of mobile and bulk soil water. Vadose Zone Journal 17: 170149.

Stocker, M.D., Pachepsky, Y.A., Hill, R.L., Shelton, D.R., 2015. Depth-dependent survival of *Escherichia coli* and Enterococci in soil after manure application and simulated rainfall. Applied and Environmental Microbiology 81: 4801-4808.

Stumpp, C., Maloszewski, P., 2010. Quantification of preferential flow and flow heterogeneities in an unsaturated soil planted with different crops using the environmental isotope $\delta^{18}O$. Journal of Hydrology 394: 407-415.

Tetzlaff, D., Capell, R., and Soulsby, C., 2012. Land use and hydroclimatic influences on Faecal Indicator Organisms in two large Scottish catchments: Towards land use-based models as screening tools. Science of the Total Environment 434: 110-122.

Thomann, R.V., Mueller, J.A., 1987. Principles of surface water quality modeling and control. Harper and Row: New York.

Vaché, K.B., McDonnell, J.J., 2006. A process-based rejectionist framework for evaluating catchment runoff model structure. Water Resources Research 42: W02409.

van Huijgevoort, M.H.J., Tetzlaff, D., Sutanudjaja, E.H., Soulsby, C., 2016. Using high resolution tracer data to constrain water storage, flux and age estimates in a spatially distributed rainfall-runoff model. Hydrological Processes 30: 4761-4778.

Vinten, A., Sample, J., Ibiyemi, A., Abdul-Salam, Y., Stutter,M., 2017. A tool for cost-effectiveness analysis of field scale sediment-bound phosphorus mitigation measures and application to analysis of spatial and temporal targeting in the Lunan Water catchment, Scotland. Science of the Total Environment 586: 631–641.

1047 Vinten, A.J.A., Sym, G., Avdic, K., Crawford, C., Duncan, A., Merrilees, D.W., 2008. Faecal indicator pollution
1048 from a dairy farm in Ayrshire, Scotland: Source apportionment, risk assessment and potential of
1049 mitigation measures. Water Research 42: 997-1012.

1050 Vivoni, E. R., 2012. Diagnosing seasonal vegetation impacts on evapotranspiration and its partitioning at the
1051 catchment scale during SMEX04–NAME. Journal of Hydrometeorology 13(5): 1631–1638.

1052 Vogel, H.-J., Weller, U., Ippisch, O., 2010. Non-equilibrium in soil hydraulic modelling. Journal of Hydrology
1053 393: 20-28.

1054 Welch, D. 1982. Dung properties and defecation characteristics in some Scottish herbivores, with and evaluation
1055 of the dung-volume method of assess occupance. Acta Theriologica 27: 191-212.

1056 Wellen, C., Kamran-Disfani, A.R., Arhonditsis, G.B., 2015. Evaluation of the current state of distributed
1057 watershed nutrient water quality modeling. Environmental Science and Technology 49: 3278-3290.

1058 Whitehead, P.G., Leckie, H., Rankinen, K., Butterfield, D., Futter, M.N., Bussi, G., 2016. An INCA model for
1059 pathogens in rivers and catchments: Model structure, sensitivity analysis and application to the River
1060 Thames catchment, UK. Science of the Total Environment 572: 1601-1610.

1061 Zhang, W., Montgomery, D.R., 1994. Digital elevation model grid size, landscape representation, and hydrologic
1062 simulations. Water Resources Research 30: 1019-1028.

1063

Figures

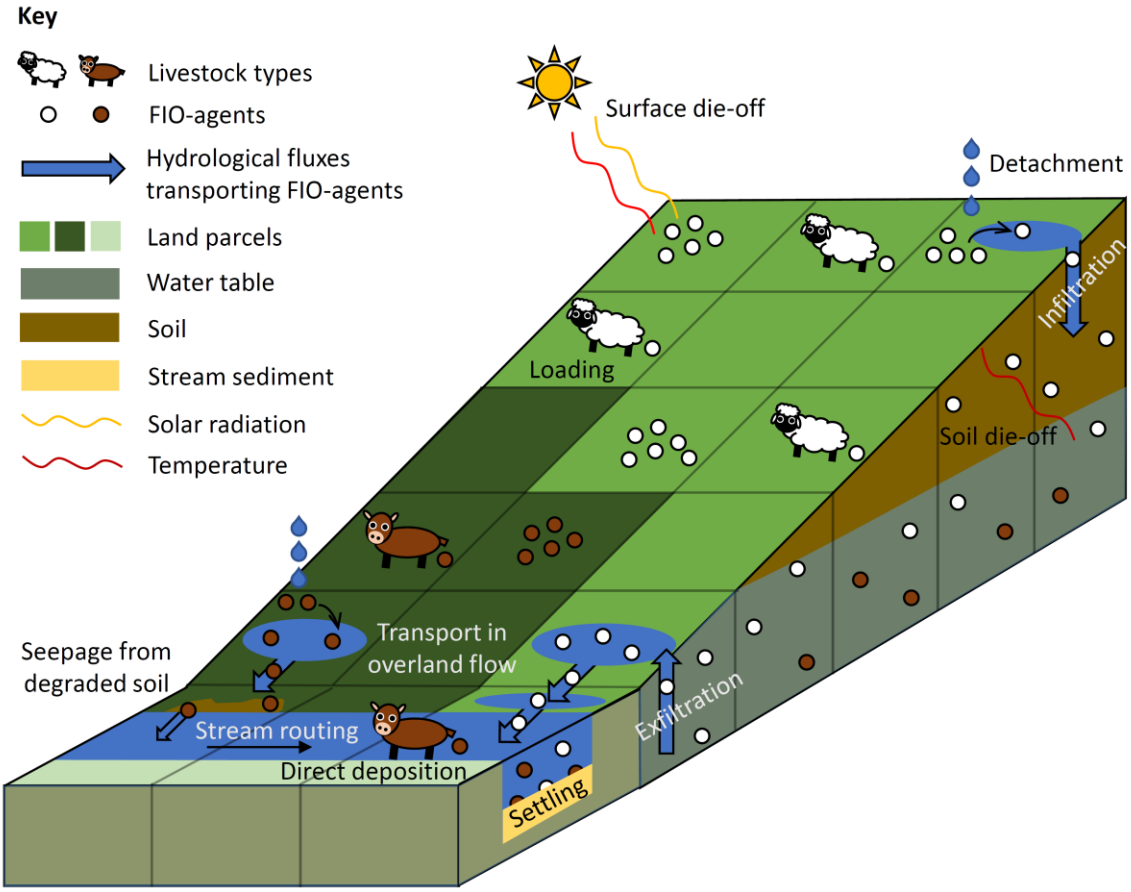

Figure 1: A conceptual diagram of MAFIO showing the faecal indicator organism (FIO) behaviour and transport processes simulated by the model. Simulations take place on a regular spatial grid.

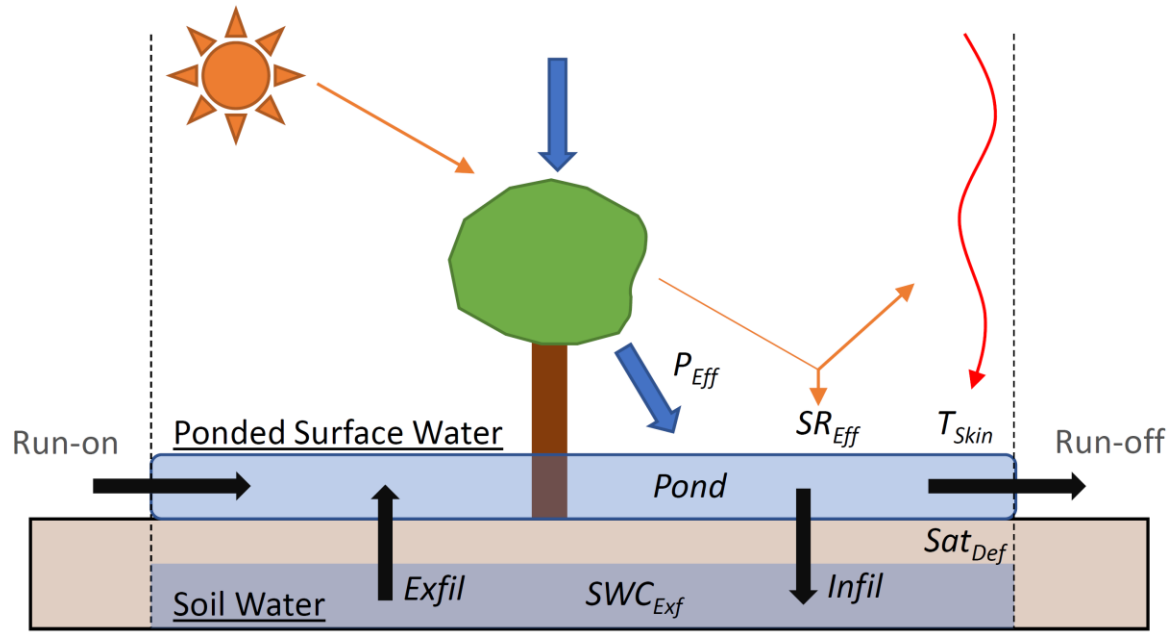

Figure 2: The abstract catchment system represented by the variables of the hydrological environment. Variables in black italic font are those provided explicitly by the hydrological environment: Effective precipitation (P_{Eff}), effective solar radiation (SR_{Eff}), soil skin temperature (T_{Skin}), exfiltration (*Exfil*), infiltration (*Infil*), ponded water prior to infiltration (*Pond*), soil water content prior to exfiltration (SWC_{Exf}) and soil saturation deficit (Sat_{Def}). Grey, non-italicised font denotes fluxes capable of affecting FIO-agent behaviour (*Run-on* and *Run-off*) that are represented implicitly. Hydrological stores are underlined. Note that *Exfil* will be non-zero if Sat_{Def} is 0 – both are shown here for illustrative purposes only.

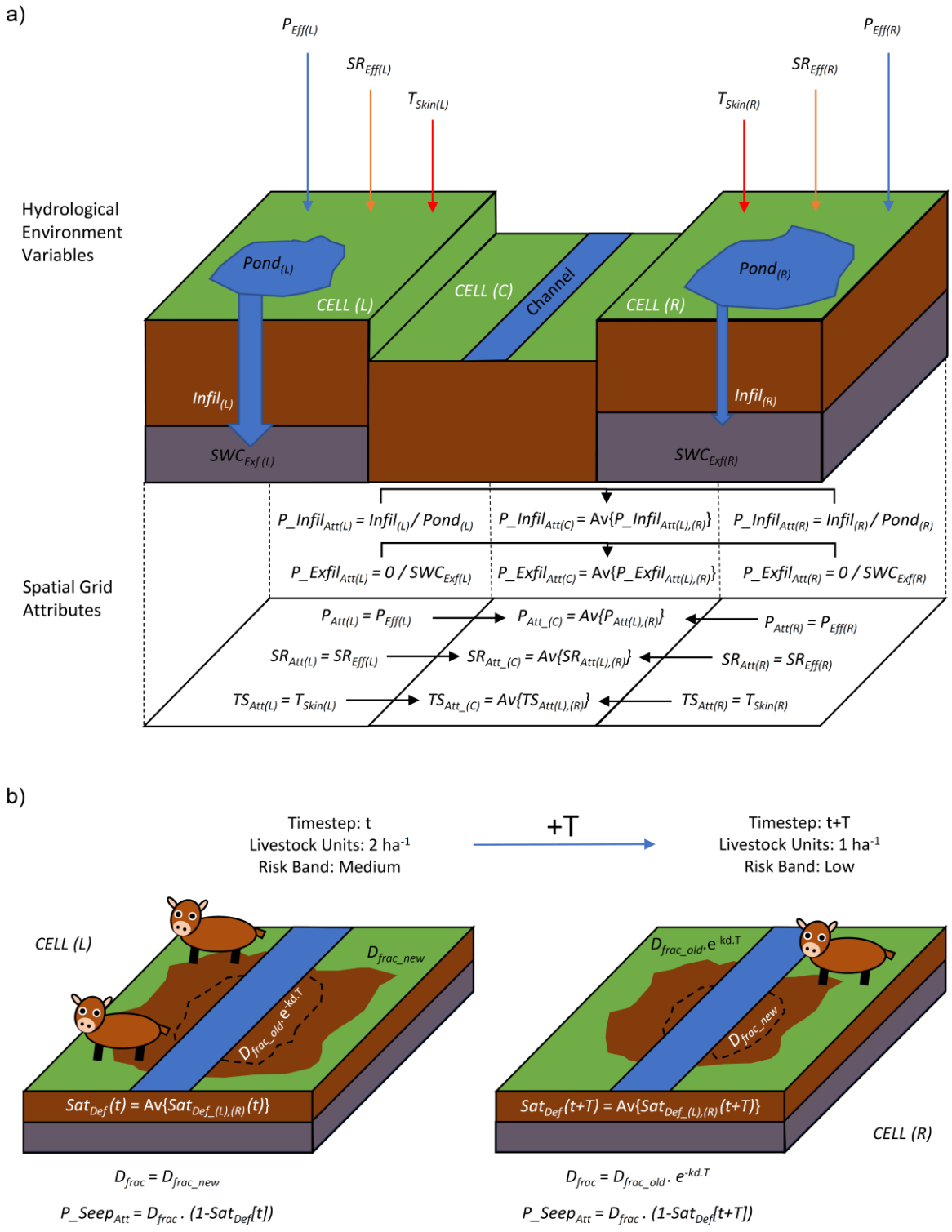

1079

1080 *Figure 3:* Examples of how attributes of the spatial grid are calculated: a) Effective precipitation (P_{Eff}),
1081 effective solar radiation (SR_{Eff}), soil skin temperature (T_{Skin}), ponded surface water prior to infiltration
1082 (*Pond*), infiltration flux (*Infil*) and soil water content prior to exfiltration (SWC_{Exf}) for two cells (L and
1083 R) of the hydrological environment are used to calculate the attributes effective precipitation (P_{Att}),
1084 effective solar radiation (SR_{Att}), soil skin temperature (TS_{Att}), probability of infiltration (P_Infil_{Att}) and

probability of exfiltration (P_Exfil_{Att}) for the corresponding cells of the spatial grid, whilst the average of these are used as the attributes of a channel cell (C) into which the cells drain; b) P_Seep_{Att} is calculated for two sequential timesteps – at timestep t, the new damage fraction (D_{frac_new}) is used in the calculation as the presence of a moderate number of livestock causes this to exceed the damage fraction from the previous timestep (D_{frac_old}) subject to exponential decay at rate k_d, whilst the reduction in livestock numbers at timestep $t+T$ causes the reverse to then be true. In a), black arrows denote how attributes/variables from cells (L) and (R) are used in determining average values for attributes/variables for cell (C).

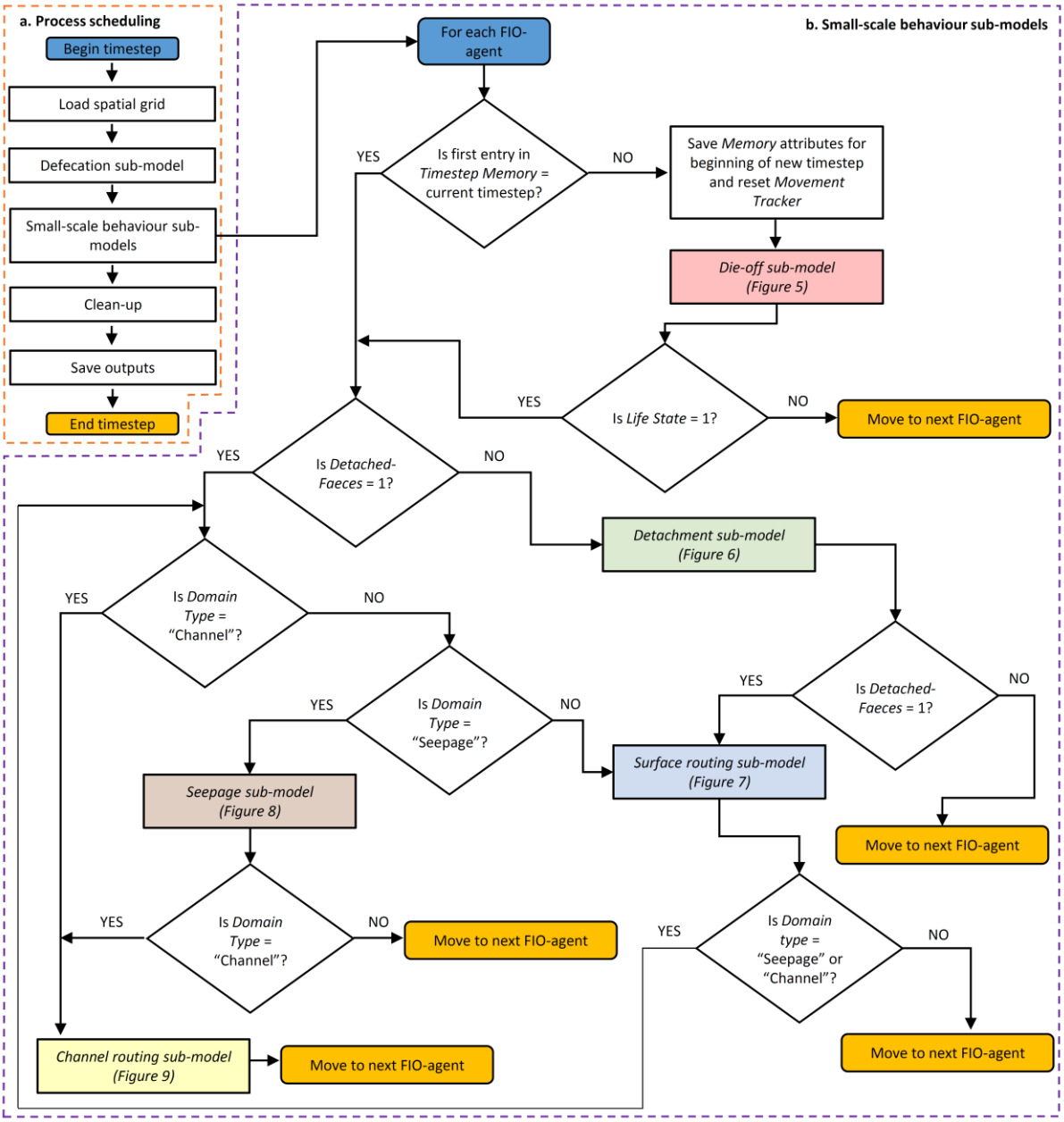

Figure 4: Flowcharts showing a) The scheduling of processes during each timestep of MAFIO; b) The sequence of small-scale behaviour sub-models that can be run for FIO-agents conditional on the values of certain attributes (indicated by underlined font). Detailed flowcharts showing the functioning of individual sub-models in b) are provided in Figures 5-9.

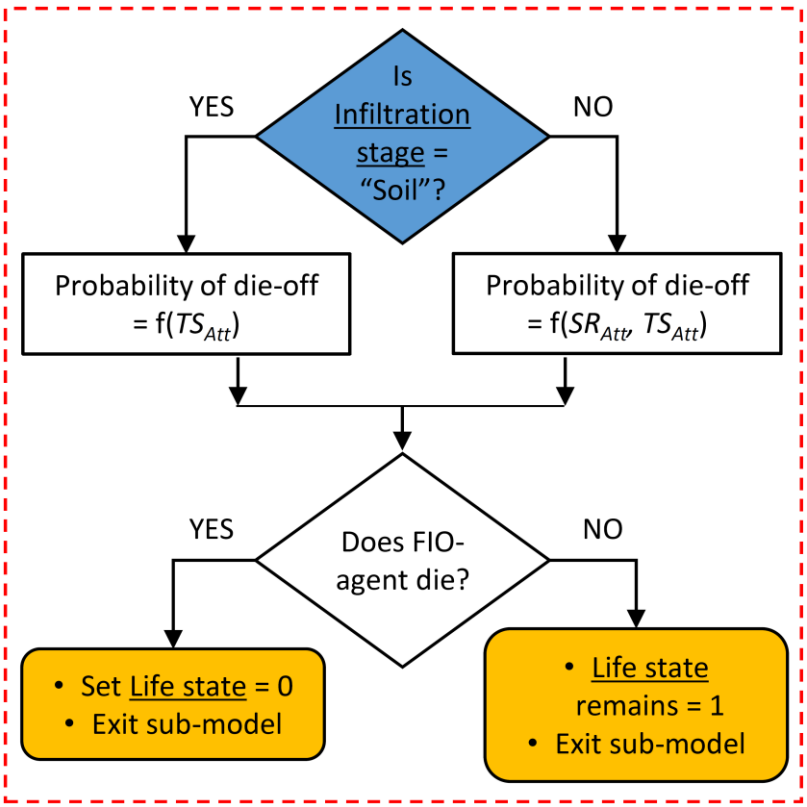

Figure 5: Detailed flowchart for the Die-off Sub-model. Attributes of the spatial grid used by the sub-model are denoted by italic font (TS_{Att} = soil skin temperature, SR_{Att} = effective solar radiation) whilst attributes of FIO-agents that are used by the sub-model are underlined. Blue shapes denote the starting operation of the sub-model whilst orange shapes denote where the sub-model can exit.

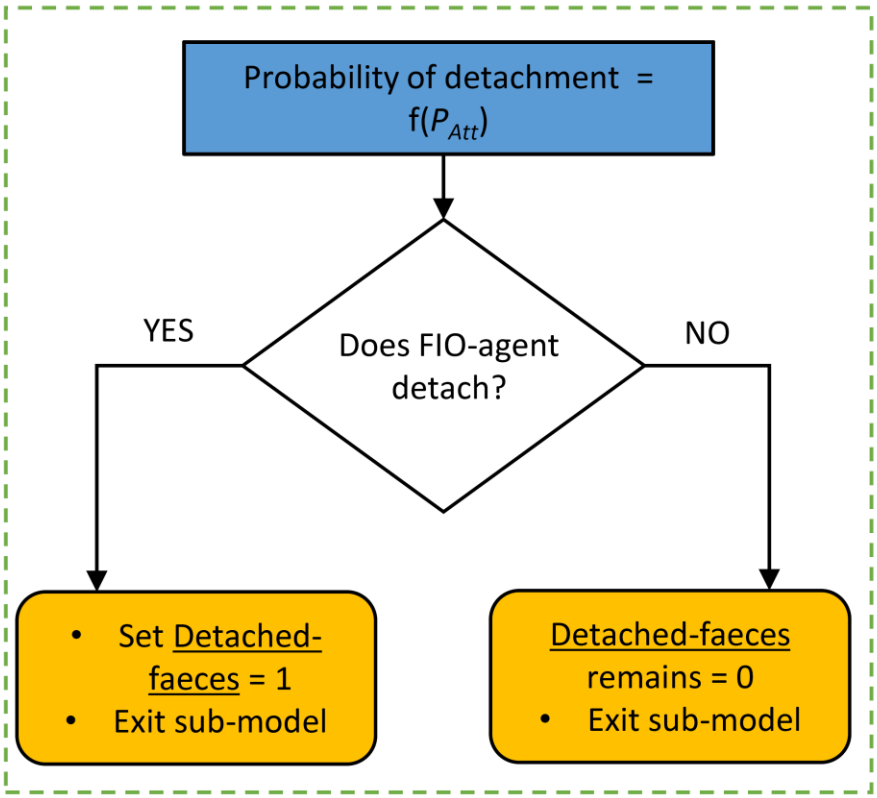

Figure 6: Detailed flowchart for the Detachment Sub-model. Attributes of the spatial grid used by the sub-model are denoted by italic font (P_{Att} = effective precipitation) whilst attributes of FIO-agents that are used by the sub-model are underlined. Blue shapes denote the starting operation of the sub-model whilst orange shapes denote where the sub-model can exit.

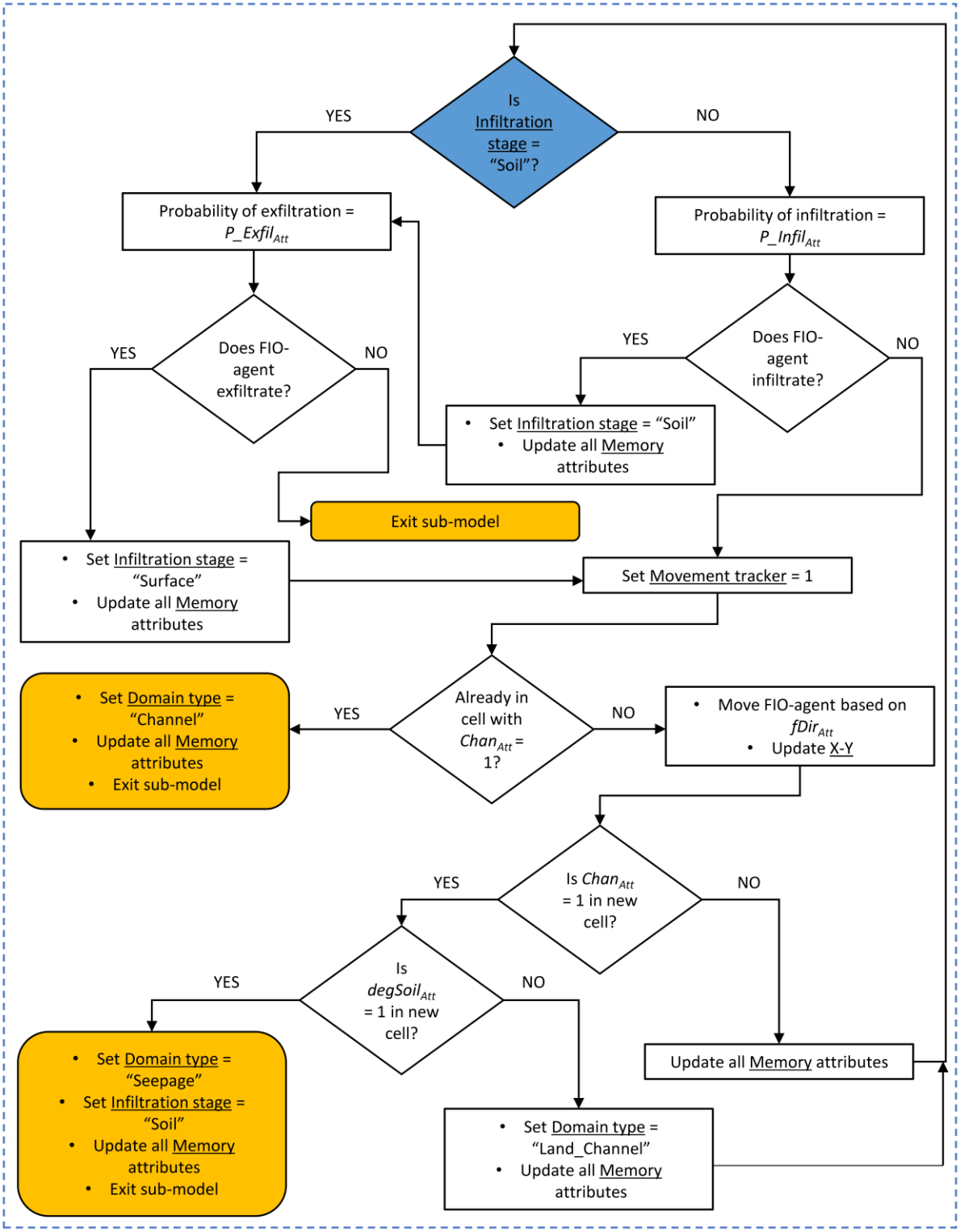

Figure 7: Detailed flowchart for the Surface Routing Sub-model. Attributes of the spatial grid used by the sub-model are denoted by italic font (P_Infil_{Att} = probability of infiltration, P_Exfil_{Att} = probability of exfiltration, $Chan_{Att}$ = channel cell, $fDir_{Att}$ = flow direction, $degSoil_{Att}$ = degraded soil in cell) whilst attributes of FIO-agents that are used by the sub-model are underlined. Blue shapes denote the starting operation of the sub-model whilst orange shapes denote where the sub-model can exit.

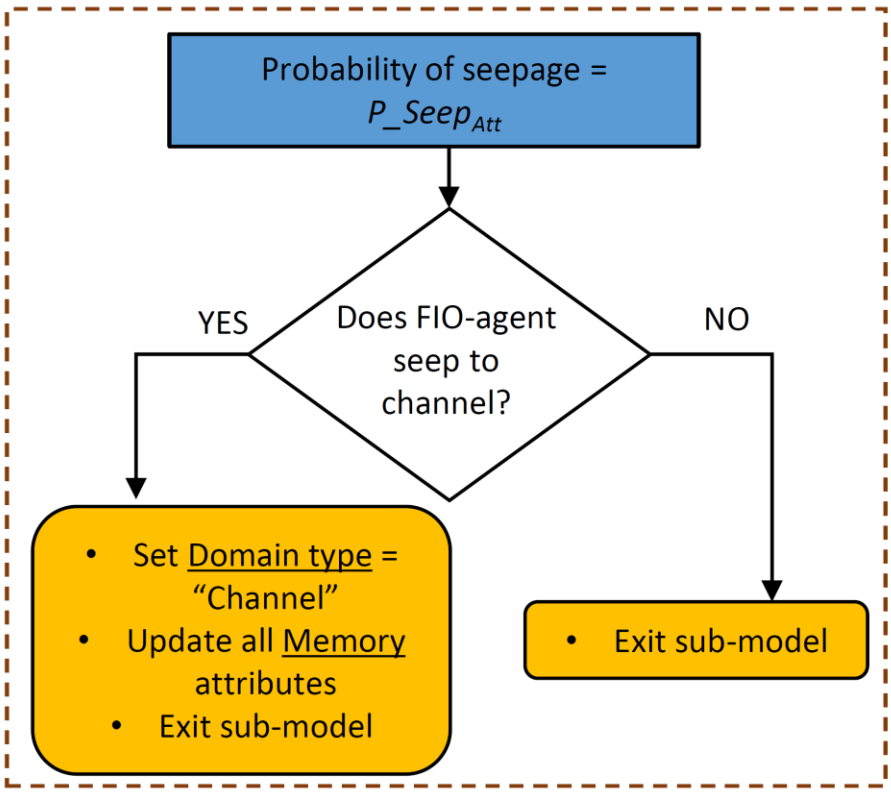

Figure 8: Detailed flowchart for the Seepage Sub-model. Attributes of the spatial grid used by the sub-model are denoted by italic font (*P_Seep*$_{Att}$ = probability of seepage) whilst attributes of FIO-agents that are used by the sub-model are underlined. Blue shapes denote the starting operation of the sub-model whilst orange shapes denote where the sub-model can exit.

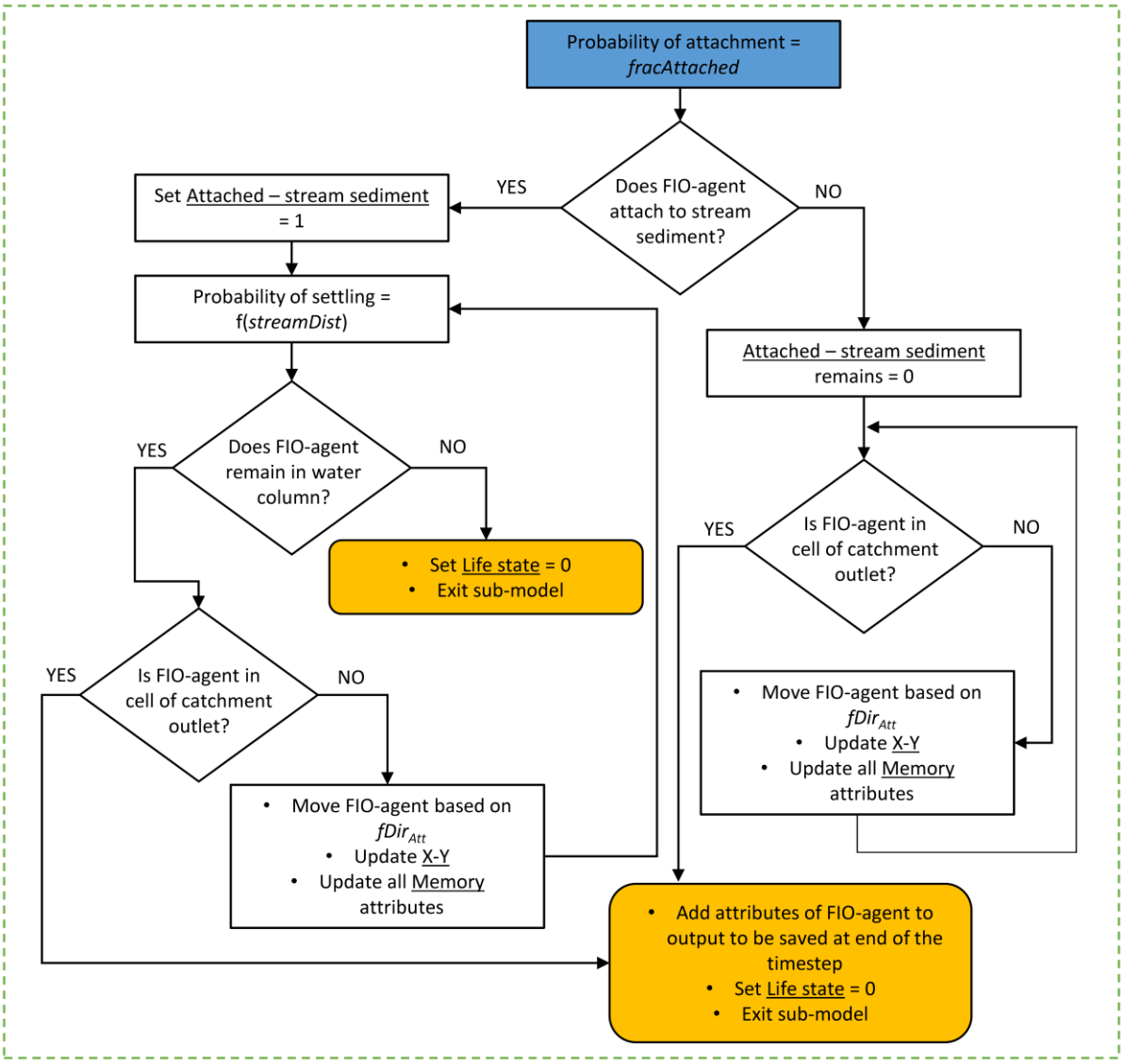

Figure 9: Detailed flowchart for the Channel Routing Sub-model. Attributes of the spatial grid used by the sub-model are denoted by italic font ($fDir_{Att}$ = flow direction); an exception is *streamDist* (straight-line length of the channel), which is derived from the flow direction and cell size attributes of the spatial grid. Attributes of FIO-agents that are used by the sub-model are underlined. *fracAttached* is a global model parameter denoting the fraction of FIOs assumed to be attached to sediment once in the stream. Blue shapes denote the starting operation of the sub-model whilst orange shapes denote where the sub-model can exit.

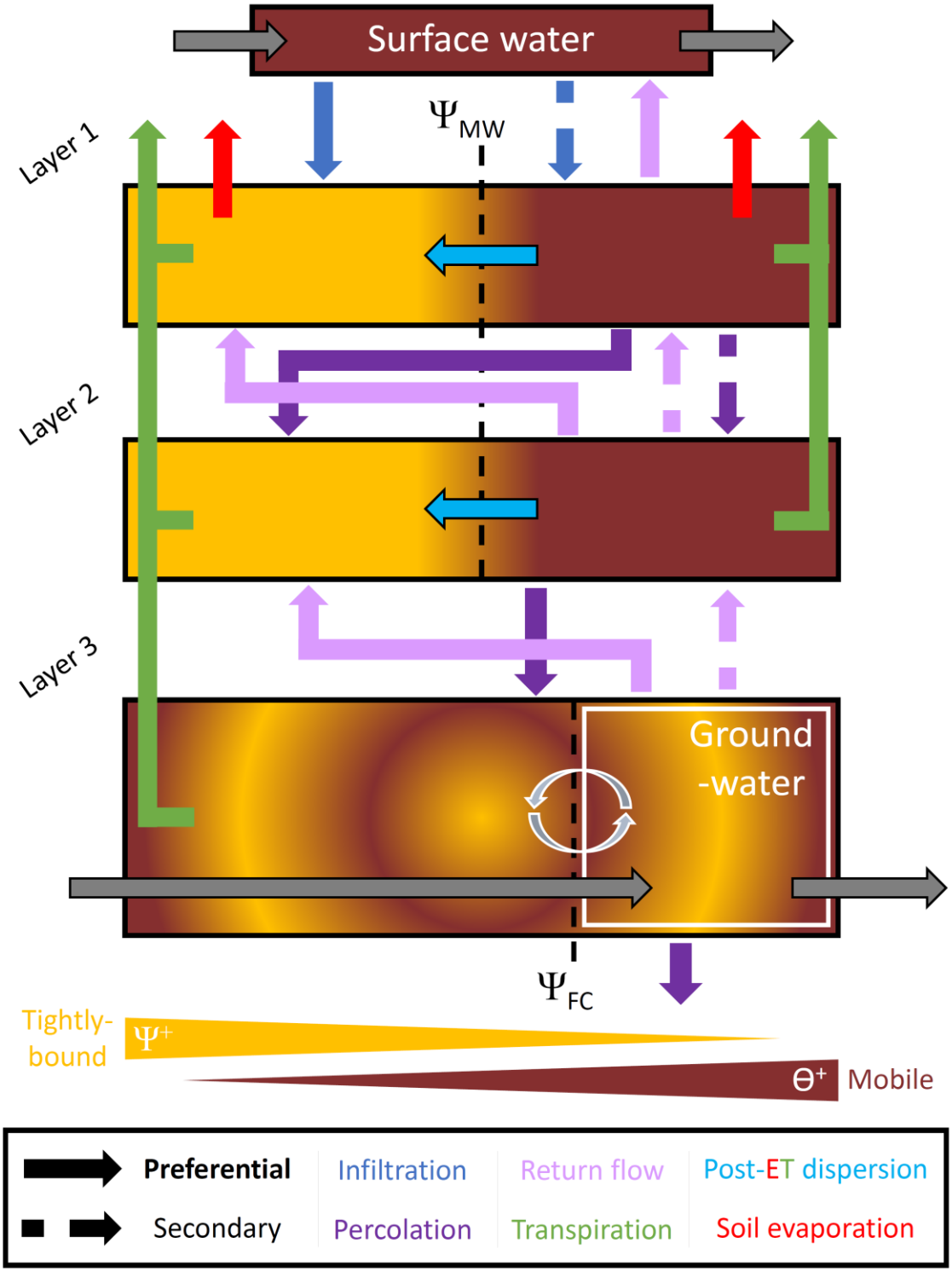

1133

1134 *Figure 10:* A conceptual graphic of the below-canopy liquid stores and new water tracking scheme in
1135 each pixel of EcH$_2$O-iso. The two-pore domain implementation (tightly-bound [TB] and mobile [MW])
1136 in Layers 1 and 2 uses a tension threshold for mobile water (Ψ_{MW}). Liquid water exchanges between
1137 layers (infiltration, percolation and return flow) follow the preferential pathways (solid arrows) unless

the recipient layer/domain is full, in which case secondary flow paths (dashed arrows) are triggered. In Layers 1 and 2, soil evaporation and plant transpiration draw from both domains in proportion to their respective water contents. Dispersion replenishes TB after evaporative losses, potentially emptying MW. The groundwater store is defined using a field capacity tension threshold (Ψ_{FC}), and tracking assumes full mixing with the non-saturated Layer 3.

Tables

Table 1: The dynamic and fixed attributes of the spatial grid. In the Description section, italics and underlining are used to show where variables of the hydrological and catchment environments, respectively, are used in the derivation of attribute values.

Spatial grid attribute	Description	Units
Dynamic		
Effective precipitation (P_{Att})	*Effective precipitation* (P_{Eff}) that reaches the surface after accounting for interception losses	cm d^{-1}
Effective solar radiation (SR_{Att})	*Effective solar radiation* (SR_{Eff}) that is absorbed by the surface after accounting for transmission losses and reflection	Ly hr^{-1}
Probability of exfiltration (P_Exfil_{Att})	The proportion of *soil water content prior to exfiltration* (SWC_{Exf}) that constitutes the *exfiltration flux* (*Exfil*) to the surface	-
Probability of infiltration (P_Infil_{Att})	The proportion of *ponded surface water prior to infiltration* (*Pond*) that constitutes the *infiltration flux* (*Infil*) into the soil	-
Probability of seepage (P_Seep_{Att})	For cells with degraded soil adjacent to a channel, the probability of seepage to the channel as a function of *soil saturation deficit* (Sat_{Def}) and livestock counts for the land parcel(s) associated with the cell	-
Soil skin temperature (TS_{Att})	*Soil skin temperature* (T_{Skin})	°C
Fixed		
Cell size ($size_{Att}$)	The length of a grid cell	Metres
Channel cell ($chan_{Att}$)	Whether (1) or not (0) a channel is present in the cell	Boolean
Degraded soil in cell ($degSoil_{Att}$)	If the cell contains a channel, whether (1) or not (0) there is an area of degraded soil surrounding the channel	Boolean
Flow direction ($fDir_{Att}$)	Identifier for the direction of steepest decent	-
Land parcel(s) (LP_{Att})	Identifier for the land parcel(s) to which the cell belongs based on its location within the catchment environment	-
Proportion of cell area occupied by channel (P_Chan_{Att})	The channel area in the cell divided by the cell area	-
X-Y location (Loc_{Att})	The spatial co-ordinates of the cell	-

1151

1152 *Table 2: The dynamic and fixed attributes of FIO-agents*

1153

FIO-agent attribute	**Description**	**Possible values**
Dynamic		
Attached-stream sediment	An abstract representation of whether the FIO-agent is attached to stream sediment once in the channel	• *0*: Not attached (*Initial value*) • *1*: Attached
Detached-faeces	An abstract representation of whether the FIO-agent is detached from a "faecal deposit"	• *0*: Not detached (*Initial value for Domain type= Land or Land_Channel*) • *1*: Detached (*Initial value for Domain type = Channel or Seepage*)
Domain type	The domain type that the FIO-agent currently occupies	• *Channel*: The FIO-agent is in a cell containing a channel, in the channel • *Land*: The FIO-agent is in a cell that does not contain a channel • *Land_Channel*: The FIO-agent is in a cell containing a channel, adjacent to the channel • *Seepage*: The FIO-agent is in a cell containing a channel, within an area of degraded soil
Infiltration stage	Denotes where the FIO-agent is within the vertical discretisation of the catchment environment	• Surface: The FIO-agent is on the land surface (*Initial value for Domain type = Land or Land_Channel)* • Soil: The FIO-agent is in the soil (*Initial value for Domain type = Seepage)*
Life state	Denotes if the FIO-agent is alive or dead	• 0: Dead • 1: Alive (*Initial value*)
Movement tracker	Tracker to record if the FIO-agent has moved on the current timestep	• 0: The FIO-agent has not moved (*Initial value)* • 1: The FIO-agent has moved

Timestep	The current timestep	• The current timestep
X co-ordinate	The X co-ordinate of the FIO-agent	• The current X co-ordinate of the FIO-agent
Y co-ordinate	The Y co-ordinate of the FIO-agent	• The current Y co-ordinate of the FIO-agent
Fixed		
Land parcel	The ID of the land parcel into which the FIO-agent initially spawned	• Land parcel ID
Livestock type	The ID of the host animal from which the FIO-agent came	• Livestock ID
Memory		
Location memory	The X-Y co-ordinates previously occupied by the FIO-agent	NA
Timestep memory	The timesteps during which the FIO-agent has been in the model domain	NA
Infiltration state memory	The history of infiltration states the FIO-agent has experienced	NA
Domain type memory	The history of domain types that the FIO-agent has occupied	NA

1165 *Table 3: The inputs required to characterise the catchment environment in MAFIO*

1166

Input	Description
Maps	
Catchment spatial extent	A binary map (1 and NaN) indicating the cells which comprise the catchment.
Cells upslope of channel	A map defining the cells which are immediately upslope of each cell containing a channel. The value of each cell is the unique channel ID of the cell containing a channel into which it drains.
Cells upslope of degraded soil	A map defining the cells which are immediately upslope of each cell containing an area of degraded soil. The value of each cell is the unique seepage ID of the cell containing degraded soil into which it drains.
Channel location	A map defining cells containing a channel. Each cell with a channel has a unique channel ID.
Channel width	A map of the channel widths for each cell containing a channel.
Degraded soil locations	A map indicating the locations of where soil adjacent to the channel is degraded. Each cell with degraded soil has a unique seepage ID.
Distribution of land parcels	A map of the land parcels in the catchment. Each land parcel has a unique ID.
Local drainage direction	A map of flow directions for each cell in the catchment based on the D8 algorithm.
Timeseries	
Livestock counts	A timeseries detailing the count(s) of each livestock type for each land parcel.
Stream access	A timeseries detailing for each unique channel ID, whether livestock from each land parcel in its list of associated land parcels have access to the stream.
Lists	
Land parcel(s) associated with degraded soil	For each unique seepage ID, a list of the land parcel(s) from which livestock can contribute to soil degradation.
Stream-associated land parcel(s)	For each unique channel ID, a list of the land parcel(s) on either side of the stream.

1167

1168

1169 *Table 4: The parameters in the sub-models of MAFIO and their initial values based on simulating E. coli for*
1170 *sheep and cattle with a daily timestep.*

1171

Parameter	**Description**	**Initial values***	**Units**	**References***
Defecation sub-model				
*faecesConc***	The concentration of FIOs per gram of faeces (wet weight)	[1.73×10^6, 4.18×10^5]	$MPN^+\ g^{-1}$	Avery et al. (unpublished data)
FWeight	The wet weight of a single defecation	[58.3, 2300]	grams	Welch (1982)^
agentsRepresent	The number of FIOs for which an FIO-agent is introduced	4.18×10^5	MPN	-
defecationsPerDay	The number of times an animal defecates per day	[16, 12]	day^{-1}	Welch (1982)
Die-off sub-model				
k_0**	Inactivation rate constant at a reference temperature of 20 ℃	[0.242, 0.090]	day^{-1}	[Moriarty et al., (2011); Himathongkham et al., (1999)]
θ**	Temperature sensitivity parameter	[1.095, 1.069]	-	[Moriarty et al., (2011); Himathongkham et al., (1999)]
α_{SR}	Proportionality constant for die-off due to solar radiation	1	-	Thomann and Mueller (1987)
Detachment sub-model				
$k_{release}$**	Rate constant for rainfall-induced detachment of FIO-agents	0.153	cm^{-1}	Blaustein et al. (2016)^
Seepage sub-model				

LUs	The number of livestock units represented by an individual animal	[0.12, 1]	LU[++]	Natural England (2013)
riskBands	The boundaries of each risk band	0 < Low ≤ 1 1 < Medium < 4 High ≥ 4	LU ha^{-1}	Oliver et al. (2009)
dFrac_Bands	The damage fractions associated with each risk band	Low: 0.43 Medium: 0.53 High: 0.72	-	Sheath and Carlson (1998)
k_d	The rate constant for damage fraction decay	0.0063	day^{-1}	Elliot et al. (2002)[^]
<u>Channel routing sub-model</u>				
fracAttached	Fraction of FIOs attached to stream sediment	0.8	-	Hipsey et al. (2008)
λ_{sed}	Distance decay rate constant	0.00037	m^{-1}	Kay and McDonald (1980)

* Values in square brackets are for [sheep, cattle]; [+] MPN: most-probable number; [++] LU: livestock units; [**] Parameter values are for *E. coli*; [^] Derived from data presented in references.

1172

1173